8

Quenching of Fluorescence

Fluorescence quenching refers to any process which decreases the fluorescence intensity of a sample. A variety of molecular interactions can result in quenching. These include excited-state reactions, molecular rearrangements, energy transfer, ground-state complex formation, and collisional quenching. In this chapter we will be concerned primarily with quenching resulting from collisional encounters between the fluorophore and quencher, which is called collisional or dynamic quenching. Static quenching is a frequent complicating factor in the analysis of quenching data, but it can also be a valuable source of information about binding between the fluorescent sample and the quencher. In addition to the processes described above, apparent quenching can occur due to the optical properties of the sample. For example, high optical densities or turbidity can result in decreased fluorescence intensities. This is a trivial type of quenching which contains little molecular information. Throughout this chapter, we will assume that such trivial effects are not the cause of the observed decreases in fluorescence intensity.

Fluorescence quenching has been widely studied both as a fundamental phenomenon and as a source of information about biochemical systems. The biochemical applications of quenching are due to the intrinsic role of molecular interactions in quenching phenomena. Both static and dynamic quenching require molecular contact between the fluorophore and quencher. In the case of collisional quenching, the quencher must diffuse to the fluorophore during the lifetime of the excited state. Upon contact, the fluorophore returns to the ground state, without emission of a photon. In general, quenching occurs without any permanent change in the molecules, that is, without a photochemical reaction. In the case of static quenching, a complex is formed between the fluorophore and the quencher, and this complex is nonfluorescent. For either static or dynamic quenching to occur, the fluorophore and quencher must be in contact. The requirement of molecular contact results in the numerous applications of quenching. For example, quenching measurements can reveal the accessibility of fluorophores to quenchers. Consider a fluorophore bound either to a protein or to a membrane. If the protein or membrane is impermeable to the quencher, and the fluorophore is located in the interior of the macromolecule, then neither collisional nor static quenching can occur. For this reason, quenching studies can be used to reveal the localization of fluorophores in proteins and membranes and the permeabilities of protons and membranes to quenchers. Additionally, the rate of collisional quenching can be used to determine the diffusion coefficient of the quencher.

It is important to recognize that the phenomenon of collisional quenching results in the expansion of the volume and distance within the solution, which affects the experimental observables. The root-mean-square distance $[\sqrt{(\overline{\Delta x^2})}]$ over which a quencher can diffuse during the lifetime of the excited state (τ) is given by $\sqrt{(\overline{\Delta x^2})} = \sqrt{(2D\tau)}$, where D is the diffusion coefficient. Consider an oxygen molecule in water at 25 °C. Its diffusion coefficient is 2.5×10^{-5} cm^2/s. During a typical fluorescence lifetime of 4 ns, the oxygen molecule can diffuse 44 Å. If the lifetime is longer, diffusion over still larger distances can be observed. For example, for lifetimes of 20 and 100 ns the average distances for oxygen diffusion are 100 Å and 224 Å, respectively. With the introduction of longer-lived probes with microsecond lifetimes (Chapter 20), diffusion over still larger distances can be observed. Hence, fluorescence quenching can reveal the diffusion of quenchers over moderately large distances which are comparable to the sizes of proteins and membranes. This situation is different from that for solvent relaxation. Spectral shifts resulting from reorientation of the solvent molecules are due primarily to the solvent shell immediately adjacent to the fluorophore.

8.1. QUENCHERS OF FLUORESCENCE

A wide variety of substances act as quenchers of fluorescence. One of the best-known collisional quenchers is molecular oxygen,[1] which quenches almost all known fluorophores. Depending upon the sample under investigation, it is frequently necessary to remove dissolved oxygen to obtain reliable measurements of the fluorescence yields or lifetimes. The mechanism by which oxygen quenches fluorescence has been the subject of debate. The most likely mechanism is that the paramagnetic oxygen causes the fluorophore to undergo intersystem crossing to the triplet state. In fluid solutions the long-lived triplets are completely quenched, so that phosphorescence is not observed. Aromatic and aliphatic amines are also efficient quenchers of most unsubstituted aromatic hydrocarbons. For example, anthracene fluorescence is effectively quenched by diethylaniline.[2] In this instance the mechanism of quenching is the formation of an excited charge-transfer complex. The excited-state fluorophore accepts an electron from the amine. In nonpolar solvents, fluorescence from the excited charge-transfer complex (exciplex)

Table 8.1. Quenchers of Fluorescence

Quencher(s)	Typical fluorophore(s)[a]	Reference(s)
Acrylamide	Tryptophan	5–7, 79
Amines	Anthracene, perylene	2, 80–85
Amines	Carbazole	86
Amine anesthetics	Perylene, anthroyloxy probes	87,88
Bromate	—	89
Bromobenzene	Many fluorophores	90
Carboxy groups	Indole	91
Chloride	Quinolinium, SPQ	92–95
Chlorinated compounds	Indoles and carbazoles	96–99
Cobalt (Co^{2+})	NBD, PPO, perylene (energy transfer for some probes)	100–105
Copper (Cu^{2+})	Anthroyloctanoic acid	106
Dimethylformamide	Indole	107
Disulfides	Tyrosine	108
Ethers	9-Arylxanthyl cations	109
Halogens	Anthracene, naphthalene, carbazole	110–125
Halogen anesthetics	Pyrene, tryptophan	126,127
Hydrogen peroxide	Tryptophan	128
Imidazole, histidine	Tryptophan	129
Iodide	Antracene	130–133
Methylmercuric chloride	Carbazole, pyrene	134,135
Nickel (Ni^{2+})	Perylene	136,137
Nitromethane and nitro compounds	Polycyclic aromatic hydrocarbons	138–144
Nitroxides	Naphthalene, Tb^{3+}, anthroyloxy probes	63,145–148
NO (nitric oxide)	Naphthalene, pyrene	149–151
Olefins	Cyanonaphthalene, 2,3-dimethylnaphthalene, pyrene	152–157
Oxygen	Most fluorophores	158–166
Peroxides	Dimethylnaphthalene	167
Picolinium nicotinamide	Tryptophan	168
Pyridine	Carbazole	169
Quinones	Aromatic hydrocarbons, chlorophyll	170,171
Silver (Ag^{+})	Perylene	172
Succinimide	Tryptophan	173,174
Thallium (Tl^{+})	Naphthylaminesulfonic acid	175
Thiocyanate	Anthracene, 5,6-benzoquinoline	176,177
Trifluoroacetamide	Tryptophan	35
Xenon		178

[a] Abbreviations: NBD, 7-Nitrobenz-2-oxa-1,3-diazol-4-yl; PPO, 2,5-diphenyl-1,3,4-oxadiazole; SPQ, 6-methoxy-*N*-(3-sulfopropyl) quinoline.

is frequently observed, and one may regard this process as an excited-state reaction rather than quenching. In polar solvents the exciplex emission is often quenched, so that the fluorophore–amine interaction appears to be that of simple quenching. While it is now known that there is a modest through-space component to almost all quenching reactions, this component is short-range (< 2 Å), so that molecular contact is a requirement for quenching.

Another type of quenching is due to heavy atoms such as iodine and bromine. Halogenated compounds such as trichloroethanol and bromobenzene also act as collisional quenchers. Quenching by the larger halogens such as bromine and iodine may be a result of intersystem crossing to an excited triplet state, promoted by spin–orbit coupling of the excited (singlet) fluorophore and the halogen.[3] Since emission from the triplet state is slow, the triplet emission is highly quenched by other processes. The quenching mechanism is probably different for chlorine-containing substances. Indole, carbazole, and their derivatives are uniquely sensitive to quenching by chlorinated hydrocarbons and by electron scavengers such as protons, histidine, cysteine, NO_3^-, fumarate, Cu^{2+}, Pb^{2+}, Cd^{2+}, and Mn^{2+}.[4] Quenching by these substances probably involves donation of an electron from the fluorophore to the quencher. Additionally, indole and tryptophan and its derivatives are quenched by acrylamide, succinimide, dichloroacetamide, dimethylformamide, pyridinium hydrochloride, imidazolium hydrochloride, methionine, Eu^{3+}, Ag^+, and Cs^+. Quenchers of protein fluorescence have been summarized in several insightful reviews.[5–7] Hence, a variety of quenchers are available for studies of protein fluorescence, especially to determine the surface accessibility of tryptophan residues and the permeation of proteins by the quenchers.

Additional quenchers include purines, pyrimidines, *N*-methylnicotinamide, and *N*-alkylpyridinium and -picolinium salts.[8,9] For example, the fluorescence of both FAD and NADH is quenched by the adenine moiety; flavin fluorescence is quenched by both static and dynamic processes,[10] whereas the quenching of dihydronicotinamide appears to be primarily dynamic.[11] These aromatic substances appear to quench by formation of charge-transfer complexes. Depending upon the precise structure involved, the ground-state complex can be reasonably stable. As a result, both static and dynamic quenching are frequently observed. A variety of other quenchers are known. These are summarized in Table 8.1, which is intended to be an overview and not a complete list. Known collisional quenchers include hydrogen peroxide, nitric oxide (NO), nitroxides, BrO_4^-, and even some olefins.

Because of the variety of substances which act as quenchers, one can frequently identify fluorophore–quencher combinations for a desired purpose. It is important to note that not all fluorophores are quenched by all the substances listed above. This fact occasionally allows selective quenching of a given fluorophore. The occurrence of quenching depends upon the mechanism, which in turn depends upon the chemical properties of the individual molecules. Detailed analysis of the mechanism of quenching is complex. In this chapter we will be concerned primarily with the type of quenching, that is, whether quenching is diffusive or static in nature. Later in this chapter, we describe biochemical applications of quenching.

8.2. THEORY OF COLLISIONAL QUENCHING

Collisional quenching of fluorescence is described by the Stern–Volmer equation,

$$\frac{F_0}{F} = 1 + k_q\tau_0[Q] = 1 + K_D[Q] \qquad [8.1]$$

In this equation, F_0 and F are the fluorescence intensities in the absence and presence of quencher, respectively, k_q is the bimolecular quenching constant, τ_0 is the lifetime of the fluorophore in the absence of quencher, and [Q] is the concentration of quencher. The Stern–Volmer quenching constant is given by $k_q\tau_0$. If the quenching is known to be dynamic, the Stern–Volmer constant will be represented by K_D. Otherwise, this constant will be described as K_{SV}.

Quenching data are usually presented as plots of F_0/F versus [Q]. This is because F_0/F is expected to be linearly dependent upon the concentration of quencher. A plot of F_0/F versus [Q] yields an intercept of 1 on the y-axis and a slope equal to K_D (Figure 8.1). Intuitively, it is useful to note that K_D^{-1} is the quencher concentration at which $F_0/F = 2$, or 50% of the intensity is quenched. A linear Stern–Volmer plot is generally indicative of a single class of fluorophores, all equally accessible to quencher. If two fluorophore populations are present, and one class is not accessible to quencher, then the Stern–Volmer plots deviate from linearity toward the x-axis. This result is frequently found for the quenching of tryptophan fluorescence in proteins by polar or charged quenchers. These molecules do not readily penetrate the hydrophobic interior of proteins, and only those tryptophan residues on the surface of the protein are quenched.

It is important to recognize that observation of a linear Stern–Volmer plot does not prove that collisional quench-

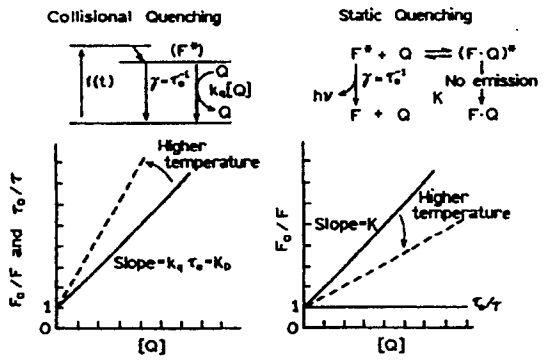

Figure 8.1. Comparison of dynamic (collisional) and static quenching.

ing of fluorescence has occurred. In Section 8.3 we will see that static quenching also results in linear Stern–Volmer plots. Static and dynamic quenching can be distinguished by their differing dependence on temperature and viscosity, or preferably by lifetime measurements. Higher temperatures result in faster diffusion and hence larger amounts of collisional quenching. Higher temperatures will typically result in the dissociation of weakly bound complexes, and hence smaller amounts of static quenching.

8.2.A. Derivation of the Stern–Volmer Equation

The Stern–Volmer equation can be derived by consideration of the fluorescence intensities observed in the absence and presence of quencher. The fluorescence intensity observed for a fluorophore is proportional to its concentration in the excited state [F*]. Under continuous illumination, a constant population of excited fluorophores is established, and therefore $d[F^*]/dt = 0$. In the absence of quencher, the differential equation describing [F*] is

$$\frac{d[F^*]}{dt} = f(t) - \gamma[F^*]_0 = 0 \qquad [8.2]$$

and in the presence of quencher,

$$\frac{d[F^*]}{dt} = f(t) - (\gamma + k_q[Q])[F^*] = 0 \qquad [8.3]$$

where $f(t)$ is the constant excitation function, and $\gamma = \tau_0^{-1}$ is the decay rate of the fluorophore in the absence of quencher. In the absence of quenching, the excited-state population decays with a rate $\gamma = (\Gamma + k_{nr})$, where Γ is the radiative decay rate and k_{nr} is the nonradiative decay rate. In the presence of quencher, there is an additional decay rate, $k_q[Q]$. With continuous excitation, the excited-state population is constant, so the derivative can be easily eliminated from these equations. Division of Eq. [8.3] by Eq. [8.2] yields

$$\frac{F_0}{F} = \frac{\gamma + k_q[Q]}{\gamma} = 1 + k_q\tau_0[Q] \qquad [8.4]$$

which is the Stern–Volmer equation.

This equation may also be obtained by considering the fraction of excited fluorophores, relative to the total, which decay by emission. This fraction (F/F_0) is given by the ratio of the decay rate in the absence of quencher (γ) to the total decay rate in the presence of quencher ($\gamma + k_q[Q]$),

$$\frac{F}{F_0} = \frac{\gamma}{\gamma + k_q[Q]} = \frac{1}{1 + K_D[Q]} \qquad [8.5]$$

which is again the Stern–Volmer equation. Since collisional quenching is a rate process which depopulates the excited state, the lifetimes in the absence (τ_0) and presence (τ) of quencher are given by

$$\tau_0 = \gamma^{-1} \qquad [8.6]$$

$$\tau = (\gamma + k_q[Q])^{-1} \qquad [8.7]$$

and therefore

$$\frac{\tau_0}{\tau} = 1 + k_q\tau_0[Q] \qquad [8.8]$$

This equation illustrates an important characteristic of collisional quenching, which is an equivalent decrease in fluorescence intensity and in lifetime (Figure 8.1, left); that is, for collisional quenching,

$$\frac{F_0}{F} = \frac{\tau_0}{\tau} \qquad [8.9]$$

The decrease in lifetime occurs because quenching is an additional rate process that depopulates the excited state. The decrease in yield occurs because quenching depopulates the excited state without fluorescence emission. Static quenching does not decrease the lifetime because only the fluorescent molecules are observed, and the uncomplexed fluorophores have the unquenched lifetime τ_0.

8.2.B. Interpretation of the Bimolecular Quenching Constant

A frequently encountered value is the bimolecular quenching constant (k_q), which can reflect the efficiency of quenching or the accessibility of the fluorophores to the quencher. As shown below, diffusion-controlled quenching typically results in values of k_q near 1×10^{10} M^{-1} s^{-1}. Smaller values of k_q can result from steric shielding of the fluorophore, and larger apparent values of k_q usually indicate some type of binding interaction.

The meaning of the bimolecular quenching constant can be understood in terms of the frequency of collisions between freely diffusing molecules. The collisional frequency (Z) of a fluorophore with a quencher is given by

$$Z = k_0[Q] \qquad [8.10]$$

where k_0 is the diffusion-controlled bimolecular rate constant. This constant may be calculated using the Smoluchowski equation,

$$k_0 = \frac{4\pi RDN}{1000} = \frac{4\pi N}{1000}(R_f + R_q)(D_f + D_q) \qquad [8.11]$$

where R is the collision radius, D is the sum of the diffusion coefficients of the fluorophore (D_f) and quencher (D_q), and N is Avogadro's number. The collision radius is generally assumed to be the sum of the molecular radii of the fluorophore (R_f) and quencher (R_q). This equation describes the diffusive flux of a molecule with a diffusion coefficient D through the surface of a sphere of radius R. The factor of 1000 is necessary to keep the units correct when the concentration is expressed in terms of molarity. The term $N/1000$ converts molarity to molecules per cubic centimeter.

The collisional frequency is related to the bimolecular quenching constant by the quenching efficiency f_Q,

$$k_q = f_Q k_0 \qquad [8.12]$$

For example, if $f_Q = 0.5$, then 50% of the collisional encounters are effective in quenching, and one expects k_q to be one-half of k_0. Since k_0 can be estimated with moderate precision, the observed value of k_q can be used to jndge the efficiency of quenching. Quenchers like oxygen, acrylamide, and I^- generally have efficiencies near unity, but the quenching efficiency of succinimide depends on the solvent. The efficiency is generally less with the lighter halogens. The quenching efficiency of amines depends upon the reduction potential of the fluorophores being quenched, as may be expected for a charge-transfer reaction.

The efficiency of quenching can be calculated from the observed value of k_q, if the diffusion coefficients and molecular radii are known. The radii can be obtained from molecular models, or from the molecular weights and densities of the substances in question. Diffusion coefficients may be obtained from the Stokes–Einstein equation,

$$D = kT/6\pi\eta R \qquad [8.13]$$

where k is the Boltzmann constant, η is the solvent viscosity, and R is the molecular radius. Frequently, the Stokes–Einstein equation underestimates the diffusion coefficients of small molecules. For example, quenching efficiencies of 2–3 were calculated for oxygen quenching of fluorophores dissolved in various alcohols.[12] These impossibly large efficiencies were obtained because the diffusion coefficient of oxygen in organic solvents is severalfold larger than predicted by Eq. [8.13]. This equation describes the diffusion of molecules that are larger than the solvent molecules, which is clearly not the case for oxygen in ethanol. As an alternative method, diffusion coefficients can be obtained from nomograms based upon physical properties of the system.[13] Once the diffusion coefficients are known, the bimolecular quenching constant for $f_Q = 1$ can be predicted using the Smoluchowski equation (Eq. [8.11]).

It is instructive to consider typical values for k_q and the concentrations of quencher required for significant quenching. For example, consider the quenching of tryptophan by oxygen.[14] At 25 °C the diffusion coefficient of oxygen in water is 2.5×10^{-5} cm^2/s and that of tryptophan is 0.66×10^{-5} cm^2/s. Assuming a collision radius of 5 Å, substitution into Eq. [8.11] yields $k_0 = 1.2 \times 10^{10}$ M^{-1} s^{-1}. The observed value of the oxygen Stern–Volmer quenching constant was 32.5 M^{-1}. Since the unquenched lifetime

of tryptophan is 2.7 ns, $k_q = 1.2 \times 10^{10}\ M^{-1}\ s^{-1}$ which is in excellent agreement with the predicted value. This indicates that essentially every collision of oxygen with tryptophan is effective in quenching, that is, $f_Q = 1.0$. A bimolecular quenching constant near $1 \times 10^{10}\ M^{-1}\ s^{-1}$ may be considered as the largest possible value in aqueous solution. For quenchers other than oxygen, smaller diffusion-limited quenching constants are expected because the diffusion coefficients of the quenchers are smaller. For example, the efficiency of acrylamide quenching of tryptophan fluorescence is also near unity,[15] but $k_q = 5.9 \times 10^9\ M^{-1}\ s^{-1}$. This somewhat smaller value of k_q is a result of the smaller diffusion coefficient of acrylamide relative to that of oxygen. Frequently, data are obtained for fluorophores which are bound to macromolecules. In this case, the fluorophore is not diffusing as rapidly. Also, the quenchers can probably only approach the fluorophores from a particular direction. In such cases, the maximum bimolecular quenching constant is expected to be about 50% of the diffusion-controlled value.[16]

8.3. THEORY OF STATIC QUENCHING

In the previous section we described quenching that resulted from diffusive encounters between the fluorophore and quencher during the lifetime of the excited state. This is a time-dependent process. Quenching can also occur as a result of the formation of a nonfluorescent complex between the fluorophore and quencher. When this complex absorbs light, it immediately returns to the ground state without emission of a photon (Figure 8.1).

The dependence of the fluorescence intensity upon quencher concentration for static quenching is easily derived by consideration of the association constant for complex formation. This constant is given by

$$K_S = \frac{[F - Q]}{[F][Q]} \qquad [8.14]$$

where [F–Q] is the concentration of the complex, [F] is the concentration of uncomplexed fluorophore, and [Q] is the concentration of quencher. If the complexed species is nonfluorescent, then the fraction of the fluorescence that remains, F/F_0, is given by the fraction of the total fluorophores that are not complexed, $f = F/F_0$. Recalling that the total concentration of fluorophore, $[F]_0$, is given by

$$[F]_0 = [F] + [F - Q] \qquad [8.15]$$

substitution into Eq. [8.14] yields

$$K_S = \frac{[F]_0 - [F]}{[F][Q]} = \frac{[F_0]}{[F][Q]} - \frac{1}{[Q]} \qquad [8.16]$$

We can substitute fluorescence intensities for the fluorophore concentrations, and rearrangement of Eq. [8.16] yields

$$\frac{F_0}{F} = 1 + K_S[Q] \qquad [8.17]$$

Note that the dependence of F_0/F on [Q] is linear and is identical to that observed for dynamic quenching except that the quenching constant is now the association constant. Unless additional information is provided, fluorescence quenching data obtained by intensity measurements alone can be explained by either a dynamic or a static process. As will be shown below, the magnitude of K_S can sometimes be used to demonstrate that dynamic quenching cannot account for the decrease in intensity. The measurement of fluorescence lifetimes is the most definitive method to distinguish static and dynamic quenching. Static quenching removes a fraction of the fluorophores from observation. The complexed fluorophores are nonfluorescent, and the only observed fluorescence is from the uncomplexed fluorophores. The uncomplexed fraction is unperturbed, and hence the lifetime is τ_0. Therefore, for static quenching $\tau_0/\tau = 1$ (Figure 8.1, right). In contrast, for dynamic quenching, $\tau_0/\tau = F_0/F$.

Besides measurement of fluorescence lifetimes, static and dynamic quenching can often be distinguished on the basis of other considerations. Dynamic quenching depends upon diffusion. Since higher temperatures result in larger diffusion coefficients, the bimolecular quenching constants are expected to increase with increasing temperature (Figure 8.1). More specifically, k_q is expected to be proportional to T/η since diffusion coefficients are proportional to this ratio (Eq. [8.13]). In contrast, increased temperature is likely to result in decreased stability of complexes, and thus lower values of the static quenching constants.

One additional method to distinguish static and dynamic quenching is by careful examination of the absorption spectra of the fluorophore. Collisional quenching only affects the excited states of the fluorophores, and thus no changes in the absorption spectra are expected. In contrast, ground-state complex formation will frequently result in perturbation of the absorption spectrum of the fluorophore. In fact, a more complete form of Eq. [8.17] would include the possibility of different extinction coefficients for the free and complexed forms of the fluorophore.

8.4. COMBINED DYNAMIC AND STATIC QUENCHING

In many instances the fluorophore can be quenched both by collisions and by complex formation with the same quencher. The characteristic feature of the Stern–Volmer plots in such circumstances is an upward curvature, concave toward the y-axis (Figure 8.2). Then the fractional fluorescence remaining (F/F_0) is given by the product of the fraction not complexed (f) and the fraction not quenched by collisional encounters. Hence,

$$\frac{F}{F_0} = f\frac{\gamma}{\gamma + k_q[Q]} \qquad [8.18]$$

In the previous section we found that $f^{-1} = 1 + K_S[Q]$. Inversion of Eq. [8.18] and rearrangement of the last term on the right yields

$$\frac{F_0}{F} = (1 + K_D[Q])(1 + K_S[Q]) \qquad [8.19]$$

This modified form of the Stern–Volmer equation is second-order in [Q], which accounts for the upward curvature observed when both static and dynamic quenching occur for the same fluorophore.

The dynamic portion of the observed quenching can be determined by lifetime measurements. That is, $\tau_0/\tau = 1 + K_D[Q]$. If lifetime measurements are not available, then Eq. [8.19] can be modified to allow a graphical separation of K_S and K_D. Multiplication of the terms in parentheses yields

$$\frac{F_0}{F} = 1 + (K_D + K_S)[Q] + K_DK_S[Q]^2 \qquad [8.20]$$

$$= 1 + K_{app}[Q] \qquad [8.21]$$

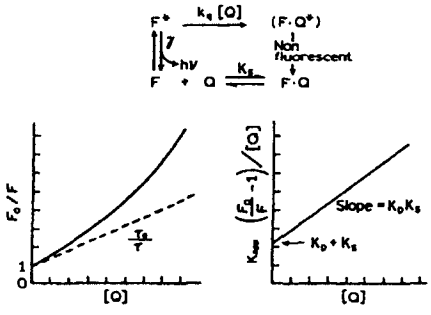

Figure 8.2. Dynamic and static quenching of the same population of fluorophores.

where

$$K_{app} = \left(\frac{F_0}{F} - 1\right)\frac{1}{[Q]} = (K_D + K_S) + K_DK_S[Q] \qquad [8.22]$$

The apparent quenching constant is calculated at each quencher concentration. A plot of K_{app} versus [Q] yields a straight line with an intercept of $K_D + K_S$ and a slope of K_DK_S (Figure 8.2). The individual values can be obtained from the two solutions of the quadratic equation obtained (see Eq. [8.23]). The dynamic component can generally be selected to be the solution comparable in magnitude to the expected diffusion-controlled value. Alternatively, the temperature or viscosity dependence of the values, or other available information, may be used as a basis for assigning the values.

8.5. EXAMPLES OF STATIC AND DYNAMIC QUENCHING

Before proceeding with additional theories and examples of quenching, it seems valuable to present some examples which illustrate both static and dynamic quenching. Data for oxygen quenching of tryptophan are shown in Figure 8.3.[14] The Stern–Volmer plot is linear, which indicates that only one type of quenching occurs. The proportional decrease in the fluorescence lifetime and yields proves that the observed quenching is due to a diffusive process. From the slope of the Stern–Volmer plot, one can calculate that $K_D = 32.5\,M^{-1}$, or that 50% of the fluorescence is quenched at an oxygen concentration of $0.031M$. The value of K_D and the fluorescence lifetime are adequate to calculate the bimolecular quenching constant, $k_q = 1.2 \times 10^{10}\,M^{-1}\,s^{-1}$. This is the value expected for the diffusion controlled bimolecular rate constant between oxygen and tryptophan (Eq. [8.11]), which indicates efficient quenching by molecular oxygen.

Static quenching is often observed if the fluorophore and quencher can have a stacking interaction. Such interactions often occur between purine and pyrimidine nucleotides and a number of fluorophores.[17–19] One example is quenching of the coumarin derivative C-120 by the nucleosides uridine (U) and deoxycytidine (dC). The intensity Stern–Volmer plot for quenching by U shows clear upward curvature (Figure 8.4). The lifetime Stern–Volmer plot is linear and shows less quenching than the intensity data. It is clear that the intensity of C-120 is being decreased by both complex formation with U as well as collisional quenching by U. Contrasting data were obtained for quenching of C-120 by dC. In this case, the Stern–Volmer plots are linear for both intensities and lifetimes, and F_0/F

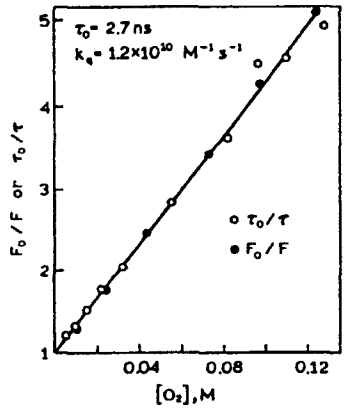

Figure 8.3. Oxygen quenching of tryptophan as observed from fluorescence lifetimes (o) and yields (•). Revised from Ref. 14.

$= \tau_0/\tau$. Hence, quenching of C-120 by dC is purely dynamic.

For quenching of C-120 by U, the static and dynamic quenching constants can be determined from a plot of K_{app} versus [U] (Figure 8.5). The slope (S) and intercept (I) were found to be 158 M^{-2} and 25.6 M^{-1}, respectively. Recalling that $I = K_D + K_S$ and $S = K_D K_S$, rearrangement yields

$$K_S^2 - K_S I + S = 0 \qquad [8.23]$$

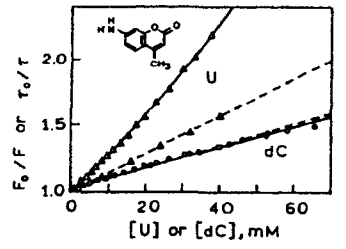

Figure 8.4. Quenching of coumarin C-120 by the nucleosides uridine (Δ, F_0/F; ▲, τ_0/τ) and deoxycytidine (O, F_0/F; •, τ_0/τ). The sample was excited at the isosbestic point at 360 nm. Revised and reprinted, with permission, from Ref. 19, Copyright © 1996, American Chemical Society.

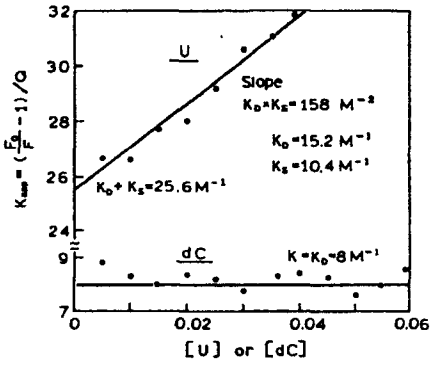

Figure 8.5. Separation of the dynamic and static quenching constants for quenching of C-120 by U or dC. Data from Ref. 19.

The solutions for this quadratic equation are K_S = 15.2 or 10.4 M^{-1}. From the lifetime data, we know that K_D is near 13.5 M^{-1}. The lower value of 10.4 M^{-1} was assigned as the static quenching constant. At a uridine concentration of 96mM, 50% of the ground state C-120 is complexed and thus nonfluorescent.

It is interesting to mention why the interactions of nucleosides and nucleotides with C-120 were studied. The goal was to develop a method for DNA sequencing using a single electrophoretic lane for all four nucleotides.[19] This would be possible if coumarin derivatives could be identified which display different lifetimes when adjacent to each nucleotide. The DNA sequence could then be determined from the lifetimes observed for each band on the sequencing gel. The use of lifetime measurements in fluorescence sensing is described in Section 19.2.B, and DNA sequencing is described in Section 21.1.

8.6. DEVIATIONS FROM THE STERN–VOLMER EQUATION; QUENCHING SPHERE OF ACTION

Positive deviations from the Stern–Volmer equation are frequently observed when the extent of quenching is large. Two examples of upward-curving Stern–Volmer plots are shown in Figures 8.6 and 8.7 for acrylamide quenching of NATA and of the fluorescent steroid dihydroequilenin (DHE), respectively. The upward-curving Stern–Volmer plots could be analyzed in terms of the static and dynamic quenching constants (Eq. [8.19]). This analysis yields K_S values near 2.8 and 5.2 M^{-1} for acrylamide quenching of

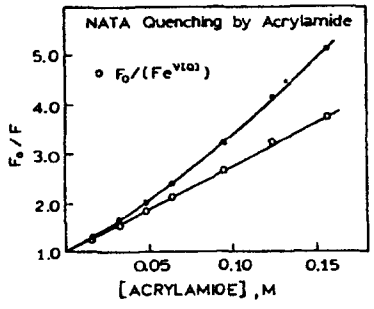

Figure 8.6. Acrylamide quenching of NATA in water. ●, F_0/F; ○, $F_0/(Fe^{V[Q]})$, where $V = 2.0\ M^{-1}$. Revised from Ref. 15.

NATA and DHE, respectively. These values imply that quencher concentrations near $0.3M$ are required to quench one-half of the fluorophores by a static process. Such a weak association suggests that the fluorophores and quenchers do not actually form a ground-state complex. Instead, it seems that the apparent static component is due to the quencher being adjacent to the fluorophore at the moment of excitation. These closely spaced fluorophore–quencher pairs are immediately quenched and thus appear to be dark complexes.

This type of apparent static quenching is usually interpreted in terms of a "sphere of action" within which the probability of quenching is unity. The modified form of the Stern–Volmer equation which describes this situation is

$$\frac{F_0}{F} = (1 + K_D[Q])\exp([Q]VN/1000) \qquad [8.24]$$

where V is the volume of the sphere.[21] The data in Figures 8.6 and 8.7 are consistent with a sphere radius near 10 Å, which is only slightly larger than the sum of the radii of

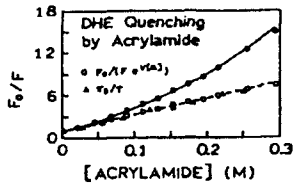

Figure 8.7. Acrylamide quenching of dihydroequilenin (DHE) in buffer containing 10% sucrose at 11 °C. ●, F_0/F; ▲, τ_0/τ; ○, $F_0/(Fe^{V[Q]})$, where $V = 2.4\ M^{-1}$. Revised and reprinted, with permission, from Ref. 20, Copyright © 1990, American Chemical Society.

the fluorophore and quencher. When the fluorophore and quencher are this close, there exists a high probability that quenching will occur before these molecules diffuse apart. As the quencher concentration increases, the probability increases that a quencher is within the first solvent shell of the fluorophore at the moment of excitation.

8.6.A. Derivation of the Quenching Sphere of Action

Assume the existence of a sphere of volume V within which the probability of immediate quenching is unity. Intuitively, if a fluorophore is excited when a quencher is immediately adjacent, then this fluorophore is quenched and is therefore unobservable. The only observable fluorophores are those for which there are no adjacent quenchers. The modified form of the Stern–Volmer equation (Eq. [8.24]) is derived by calculating the fraction of fluorophores which do not contain a quencher within their surrounding sphere of action.[21]

The Poisson probability distribution states that the probability of finding a volume V with n quenchers is

$$P(n) = \frac{\lambda^n}{n!}e^{-\lambda} \qquad [8.25]$$

where λ is the mean number of quenchers per volume V. The average concentration of quenchers (in molecules/cm^3) is given by $[Q]N/1000$, and hence the average number of molecules in the sphere is $\lambda = V[Q]N/1000$. Only those fluorophores without nearby quenchers are fluorescent. The probability that no quenchers are nearby is

$$P(0) = e^{-\lambda} \qquad [8.26]$$

Thus, the existence of the sphere of action reduces the proportion of observable fluorophores by the factor $\exp(-V[Q]N/1000)$, which in turn yields Eq. [8.24]. Division of the values of F_0/F by $\exp(V[Q]N/1000)$ corrects the steady-state intensities for this effect and reveals the dynamic portion of the observed quenching (Figures 8.6 and 8.7). For simplicity, the static term is often expressed in terms of reciprocal concentration.

8.7. EFFECTS OF STERIC SHIELDING AND CHARGE ON QUENCHING

The extent of quenching can be affected by the environment surrounding the fluorophore. One example is the quenching of the steroid DHE by acrylamide. When free in solution, DHE is readily quenched by acrylamide. How-

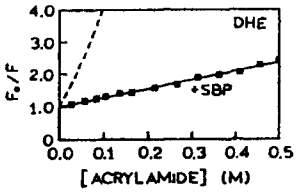

Figure 8.8. Acrylamide quenching of DHE when free in solution (—) and when bound to steroid binding protein (SBP; ■). Revised and reprinted, with permission, from Ref. 20, Copyright © 1990, American Chemical Society.

ever, when bound to a steroid binding protein (SBP), much less quenching occurs (Figure 8.8). In fact, the modest amount of quenching observed was attributed to dissociation of DHE from the protein.[20] Protection from quenching is frequently observed for probes bound to macromolecules[22,23] and even cyclodextrins.[24] In fact, binding of probes to cyclodextrins has been used as a means of obtaining room-temperature phosphorescence.[25] The macromolecules or cyclodextrins provide protection from the solvent but usually not complete protection from diffusing quenchers. Such solutions are usually purged to remove dissolved oxygen in order to observe phosphorescence.

The electronic charge on the quenchers can also have a dramatic effect on the extent of quenching (Figure 8.9). This is illustrated by quenching of 1-ethylpyrene (EP) in micelles, where the detergent molecules have different charges.[26] The quencher was *p*-*N*,*N*-dimethylaniline sulfonate (DMAS), which is negatively charged. The micelles were positively charged [dodecyltrimethylammonium chloride (DTAC)], neutral (Brij 35), or negatively charged [sodium dodecyl sulfate (SDS)]. There is extensive quenching of EP in the positively charged DTAC micelles, and essentially no quenching in the negatively charged SDS micelles. In general, one can expect charge effects to be present with charged quenchers such as iodide and to be absent for neutral quenchers like oxygen and acrylamide.

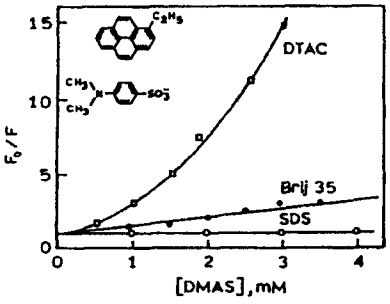

Figure 8.9. Quenching of 1-ethylpyrene (EP) by *p*-*N*,*N*-dimethylaniline sulfonate (DMAS), in positively charged micelles of dodecyltrimethylammonium chloride (DTAC), neutral micelles of Brij 35, or negatively charged micelles of sodium dodecyl sulfate (SDS). Revised from Ref. 26.

8.7.A. Accessibility of DNA-Bound Probes to Quenchers

The most dramatic effects of charge and shielding on quenching have been observed for fluorophores bound to DNA. One can expect the extent of quenching to be decreased by intercalation of probes into the DNA double helix. For instance, EB bound to DNA was found to be protected from oxygen quenching by a factor of 30 as compared to EB in solution.[14] Given the high negative charge density of DNA, one can expect the quenching to be sensitive to the charge of the quencher, the ionic strength of the solution, and the rate of quencher diffusion near the DNA helix.[27,28]

Collisional quenching by oxygen was used to study quenching of several DNA-bound probes.[29,30] Oxygen was chosen as the quencher because it is neutral and should thus be unaffected by the charge on the DNA. The probes were selected to have different sizes and different modes of binding to DNA (Figure 8.10). Proflavine intercalates into double-helical DNA and was expected to be protected from quenching. In fact, the bimolecular quenching constant was less than 10% of the diffusion-controlled rate

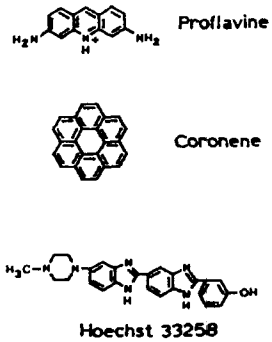

Figure 8.10. Structure of three probes bound to DNA (Table 8.2). From Ref. 30.

Table 8.2. Decay Times and Oxygen Quenching Constants of Probes Bound to DNA[a]

Fluorophore	Type of complex	τ_0 (ns)	k_q (M^{-1} s^{-1})
Proflavine	Intercalation	6.3	$<0.1 \times 10^{10}$
Coronene	Partial intercalation	225	0.17×10^{10}
Hoechst 33258	Minor groove	3.5	1.1×10^{10}

[a]Ref. 30.

(Table 8.2). The k_q value for proflavine may be smaller than shown, as there was little quenching under these experimental conditions. Hoechst 33258 is known to bind to the minor groove of DNA. Surprisingly, the k_q value for Hoechst 33258 bound to DNA was near the diffusion-controlled limit, suggesting complete accessibility by oxygen. The behavior of coronene was intermediate. Coronene is rather large and not able to fully fit into a DNA helix. The intermediate value of k_q, reflecting partial exposure to water, was explained as due to partial intercalation of coronene. These results illustrate how the extent of probe exposure can be correlated with the bimolecular quenching constant. Knowledge of the unquenched fluorescence lifetimes was essential for calculating the values of k_q from the Stern–Volmer quenching constants.

The extent of quenching can also be affected by the charge on the quenchers. This is illustrated by iodide quenching of Hoechst 33258 when free in solution and when bound to DNA (Figure 8.11). Hoechst 33258 is readily quenched by iodide when free in solution but is not quenched when bound to DNA. In the previous paragraph we saw that Hoechst 33258 bound to DNA was completely accessible to the neutral quencher oxygen. Apparently, the negative charges on DNA prevent iodide from coming into contact with Hoechst 33258 when bound to the minor groove of DNA.

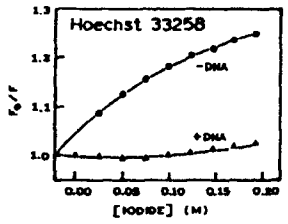

Figure 8.11. Iodide quenching of Hoechst 33258 in the absence (●) and presence (▲) of calf thymus DNA. The ionic strength was kept constant using KCl. Revised from Ref. 31.

8.7.B. Quenching of Ethenoadenine Derivatives

The nucleotide bases of DNA are mostly nonfluorescent. Fluorescent analogs of adenine nucleotides have been created by addition of an etheno bridge, the so-called ε-ATP derivatives (Chapter 3). Depending on the pH and extent of phosphorylation, the charge on the ethenoadenine nucleotides ranges from −3 for ε-ATP to 0 for ethenoadenosine. Hence, one expects the extent of quenching to depend on the charge of the quencher.

Stern–Volmer plots for the various ethenoadenine nucleotides are shown in Figure 8.12. For the neutral quencher acrylamide, there is no effect of charge. For the positively charged quencher Tl^+, the largest Stern–Volmer constant was observed for ε-ATP, with progressively smaller values as the number of negatively charged phosphates decreased. The opposite trend was observed for iodide quenching. Such effects of charge on quenching can be used to determine the local charge around fluorophores on proteins based on quenching by positive, neutral, and negatively charged quenchers.[32–34]

8.8. FRACTIONAL ACCESSIBILITY TO QUENCHERS

Proteins usually contain several tryptophan residues that are in distinct environments. Each residue can be differently accessible to quencher. Hence, one can expect complex Stern–Volmer plots and even spectral shifts due to selective quenching of exposed versus buried tryptophan residues. One example is quenching of lysozyme. This protein from egg white has six tryptophan residues, several of which are known to be near the active site. Lysozyme fluorescence was measured as a function of the concentration of trifluoroacetamide (TFA), which was found to be a collisional quencher of the fluorescence.[35] The Stern–Volmer plot curves downward toward the x-axis (Figure 8.13, left). As will be described below, this is a characteristic feature of two fluorophore populations, one of which is not accessible to the quencher. In the case of lysozyme, the emission spectrum shifts progressively to shorter wavelengths with increasing TFA concentration (Figure 8.13, right). This indicates that those tryptophan residues emitting at longer wavelengths are quenched more readily than the shorter-wavelength tryptophans.

The emission spectrum of the quenched residues can be calculated by taking the difference between the unquenched and quenched emission spectra. This difference spectrum (Figure 8.13, right) shows that the quenched residues display an emission maximum at 348 nm. The

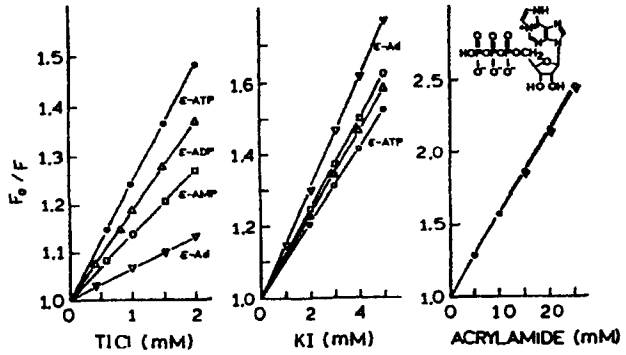

Figure 8.12. Quenching of (ε-ATP (○), ε-ADP (△), ε-AMP (□), and ε-Ad (▽) by Tl^+ (*left*), I^- (*middle*), and acrylamide (*right*) in 10m*M* phosphate buffer, 0.1*M* KCl, 20 °C, pH 7.0. Revised from Ref. 34.

protected residues display an emission maximum at 333 nm.

8.8.A. Modified Stern–Volmer Plots

The differing accessibilities of tryptophan residues in proteins have resulted in the frequent use of quenching to resolve the accessible and inaccessible residues.[36] Suppose that there are two populations of fluorophores, one being accessible (a) to quenchers and the other being inaccessible or buried (b). In this case the Stern–Volmer plot will display downward curvature (Figure 8.13). The total fluorescence in the absence of quencher (F_0) is given by

$$F_0 = F_{0a} + F_{0b} \qquad [8.27]$$

where the 0 subscript once again refers to the fluorescence intensity in the absence of quencher. In the presence of quencher, the intensity of the accessible fraction (f_a) is decreased according to the Stern–Volmer equation, whereas the buried fraction is not quenched. Therefore, the observed intensity is given by

$$F = \frac{F_{0a}}{1 + K_a[Q]} + F_{0b} \qquad [8.28]$$

where K_a is the Stern–Volmer quenching constant of the accessible fraction and [Q] is the concentration of quencher. Subtraction of Eq. [8.28] from Eq. [8.27] yields

$$\Delta F = F_0 - F = F_{0a}\left(\frac{K_a[Q]}{1 + K_a[Q]}\right) \qquad [8.29]$$

Inversion of Eq. [8.29] followed by division into Eq. [8.27] yields

$$\frac{F_0}{\Delta F} = \frac{1}{f_a K_a[Q]} + \frac{1}{f_a} \qquad [8.30]$$

where f_a is the fraction of the initial fluorescence which is accessible to quencher,

$$f_a = \frac{F_{0a}}{F_{0b} + F_{0a}} \qquad [8.31]$$

This modified form of the Stern–Volmer equation allows f_a and K_a to be determined graphically (Figure 8.14). A plot

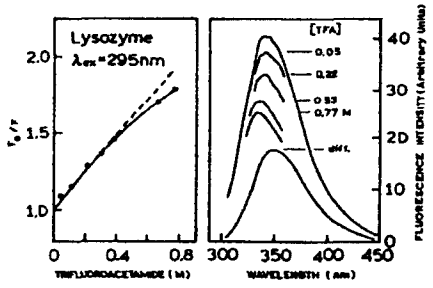

Figure 8.13. Quenching of lysozyme by trifluoroacetamide (TFA). *Left*: Stern–Volmer plot. *Right*: Emission spectra with increasing concentrations of TFA. Also shown is the difference spectrum (diff), 0.0*M* – 0.77*M* TFA. Revised and reprinted from Ref. 35, Copyright © 1984, with permission from Elsevier Science.

of $F_0/\Delta F$ versus $1/[Q]$ yields f_a^{-1} as the intercept and $(f_aK_a)^{-1}$ as the slope. A y-intercept of f_a^{-1} may be understood intuitively. The intercept represents the extrapolation to infinite quencher concentration ($1/[Q] = 0$). The value of $F_0/(F_0 - F)$ at this quencher concentration represents the reciprocal of the fluorescence which was quenched. At high quencher concentration, only the inaccessible residues will be fluorescent.

In separation of the accessible and inaccessible fractions of the total fluorescence, it should be realized that there may be more than two classes of tryptophan residues. Also, even the presumed "inaccessible" fraction may be partially accessible to quencher. This possibility is illustrated by the dashed curves in Figure 8.14, which show the expected result if the Stern–Volmer constant for the buried fraction (K_b) is one-tenth of that for the accessible fraction ($K_b = 0.1K_a$). For a limited range of quencher concentrations, the modified Stern–Volmer plot can still appear to be linear. The extrapolated value of f_a would represent an apparent value somewhat larger than seen with $K_b = 0$. Hence, the modified Stern–Volmer plots provide a useful but arbitrary resolution of two assumed classes of tryptophan residues.

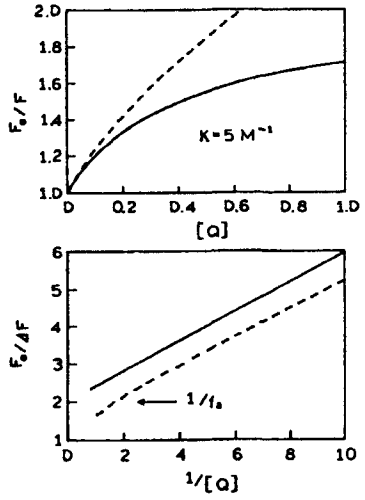

Figure 8.14. Stern–Volmer (*top*) and modified Stern–Volmer plots (*bottom*) for two populations of fluorophores, one of which is inaccessible to quencher. The dashed curves show the effect of the "inaccessible" population being quenched with a K value one-tenth of that for the accessible population.

8.8.B. Experimental Considerations in Quenching

Although quenching experiments are straightforward, there are several potential problems. One should always examine the emission spectra under conditions of maximum quenching. As the intensity is decreased, the contribution from background fluorescence may begin to be significant. Quenchers are often used at high concentrations, and the quenchers themselves may contain fluorescent impurities. Also, the intensity of the Raman and Rayleigh scatter peaks is independent of quencher concentration. Hence, the relative contribution of scattered light always increases with quenching.

It is also important to consider the absorption spectra of the quenchers. Iodide and acrylamide absorb light below 290 nm. The inner filter effect due to their absorption can decrease the apparent fluorescence intensity and thereby distort the quenching data. Regardless of the quencher being used, it is important to determine if the inner filter effects are significant. If inner filter effects are present, the observed fluorescence intensities must be corrected. The lifetime measurements are mostly independent of inner filter effects because these measurements are relatively independent of total intensity.

When iodide or other ionic quenchers are used, it is important to maintain a constant ionic strength. This is usually accomplished by addition of KCl. When iodide is used, it is also necessary to add a reducing agent such as $Na_2S_2O_3$. Otherwise, I_2 is formed, which is reactive and can partition into the nonpolar regions of proteins and membranes.

8.9. APPLICATIONS OF QUENCHING TO PROTEINS

8.9.A. Fractional Accessibility of Tryptophan Residues in Endonuclease III

Since the pioneering study of lysozyme quenching,[36] there have been numerous publications on determining the fraction of protein fluorescence accessible to quenchers.[37–41] In Section 16.5 we show that proteins in the native state often display a fraction of the emission which is not accessible to water-soluble quenchers and that denaturation of the proteins usually results in accessibility of all the tryptophan residues to quenchers. The possibility of buried and exposed residues in a single protein is illustrated by endonuclease III (endo III). Endo III is a DNA repair enzyme which displays both *N*-glycosylase and apurinine/apyrimidinic lyase activities. The structure of

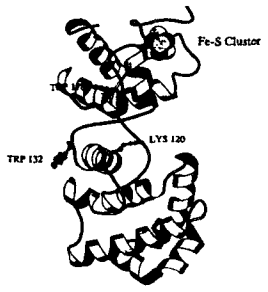

Figure 8.15. Structure of endo III, showing the exposed residue trp-132 and the buried residue trp-178 near the iron–sulfur cluster. Courtesy of Dr. Charles R. Scholes.

endo III shows two domains, with the DNA binding site in the cleft region. Endo III contains two tryptophan residues.[40] Trp-132 is exposed to the solvent, and trp-178 is buried in one of the domains (Figure 8.15). Hence, one expects these residues to be differently accessible to water-soluble quenchers.

The modified Stern–Volmer plot for quenching of endo III by iodide shows clear evidence for a shielded fraction (Figure 8.16). Extrapolation to high iodide concentrations yields an intercept near 2, indicating that only half of the emission can be quenched by iodide. This suggests that both trp residues in endo III are equally fluorescent and that only one residue (trp-132) can be quenched by iodide. Similar results have been obtained for a large number of proteins, and the extent of quenching is known to depend on the size and polarity of the quenchers.[6,7] Quenching of solvent-exposed residues in proteins is now a standard tool in the characterization of proteins.

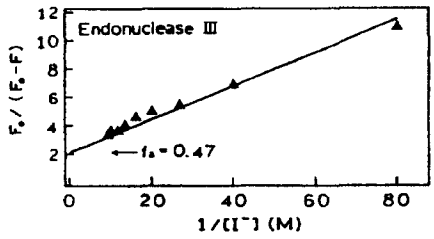

Figure 8.16. Modified Stern–Volmer plot for iodide quenching of endo III, showing evidence for two types of tryptophan residues. The inaccessible fraction is $f_a = 0.47$. Revised from Ref. 40.

8.9.B. Effect of Conformational Changes on Tryptophan Accessibility

The conformational state of a protein can have an influence on the exposure of its tryptophan residues to solvent. This is illustrated by the cyclic AMP receptor protein (CRP) from *Escherichia coli*.[41] This protein regulates the expression of over 20 genes in *E. coli*. CRP consists of two identical polypeptide chains, each containing 209 amino acids. It contains two nonidentical trp residues at positions 13 and 85.

Stern–Volmer plots for the quenching of CRP by acrylamide in the absence and in the presence of bound cyclic AMP (cAMP) are shown in Figure 8.17. In the absence of cAMP, the Stern–Volmer plot shows obvious downward curvature, indicating that one of the trp residues is inaccessible or only slightly accessible to acrylamide. Binding of cAMP results in a dramatic change in the Stern–Volmer plot, which becomes linear. Apparently, binding of cAMP to the CRP causes a dramatic conformational change which results in exposure of the previously shielded trp residue. Changes in accessibility due to conformational changes have been reported for other proteins.[42] Binding of substrates to proteins can also result in shielding of tryptophan, as has been observed for lysozyme[36] and for wheat germ agglutinin.[35]

8.9.C. Quenching of the Multiple Decay Times of Proteins

The intensity decays of proteins are typically multiexponential. Hence, it is natural to follow the individual decay times as the protein is exposed to increasing concentrations of quencher. One example is provided by the investigation of the CRP protein just described.[41] FD data for its intrinsic tryptophan emission yield decay times near 1.5 and 6.8 ns.

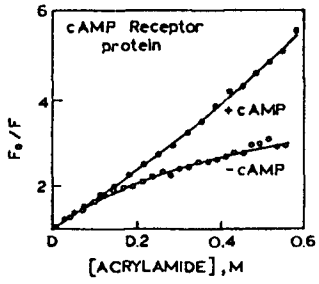

Figure 8.17 Stern–Volmer plot for acrylamide quenching of cAMP receptor protein in the absence (o) and in the presence (●) of cAMP. Revised from Ref. 41.

Similar decay times were observed in the absence and the presence of bound cAMP. For the protein without bound cAMP, the shorter decay time did not change with increasing iodide concentration (Figure 8.18, top), whereas the long lifetime decreased. This indicates that the 6.8-ns component is due to the exposed trp residue. The 1.5-ns component is not quenched by iodide and is assigned to the buried trp residue. In the presence of bound cAMP, both decay times are seen to decrease in the presence of iodide, indicating that both are quenched (Figure 8.18, bottom). These results agree with the linear Stern–Volmer plot found for CRP with bound cAMP (Figure 8.17).

While the results presented in Figure 8.18 show a clear separation of decay times, caution is needed when interpreting decay times in the presence of quencher. For many proteins, the decay times will be closer than 1.5 and 6.8 ns, and the decay time for each trp residue can depend on emission wavelength. Hence, it may not be possible to assign a unique decay time to each tryptophan residue. Additionally, collisional quenching results in nonexponential decays, even if the fluorophore shows a single decay time in the absence of quencher. This change in the intensity decay is due to transient effects in quenching, which are due to the rapid quenching of closely spaced flourophore–quencher pairs, followed by a slower quenching rate due to quencher diffusion. The presence of transient effects results in additional nanosecond decay times. The apparent lifetimes for each residue will be weighted averages that depend on the method of measurement. The assignment of decay times to trp residues in the presence of quenching can be ambiguous. Transient effects in quenching are described in the following chapter.

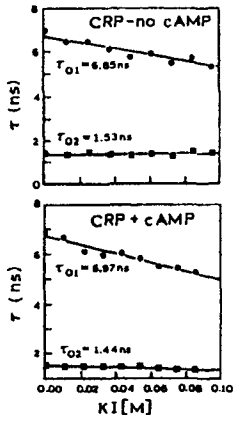

Figure 8.18. Iodide-dependent decay times of CRP in the absence (*top*) and in the presence (*bottom*) of bound cAMP. Revised from Ref. 41.

8.9.D. Effects of Quenchers on Proteins

When one performs quenching experiments, it is important to consider whether the quencher has an adverse effect on the protein. Some quenchers, such as 2,2,2-trichloroethanol, are known to bind to proteins and induce conformational changes.[43] For a time it was thought that acrylamide bound to proteins, but it is now accepted that such binding does not occur except in several specific cases.[44–46] However, even the nonperturbing quencher acrylamide can affect certain proteins, as was found for glyceraldehyde-3-phosphate dehydrogenase (GAPDH).[47] This protein contains three tryptophan residues in each subunit of the tetrameric enzyme. Quenching of the apoenzyme, which lacks NAD^+, by acrylamide yields a Stern–Volmer plot that is highly unusual. The extent of quenching increases rapidly above 0.4*M* acrylamide (Figure 8.19). This effect is not seen for the holoenzyme, which contains bound NAD^+. Acrylamide also caused a slow loss of activity and reduction in the number of thiol groups. Acrylamide appears to bind to GAPDH, reacting with the protein and destroying its activity.

8.9.E. Protein Folding of Colicin E1 • Advanced Topic •

Colicin E1 is a 522-residue polypeptide which is lethal to strains of *E. coli* that do not contain the resistance plasmid. Colicin E1 exerts its toxic effects by forming a channel in the cytoplasmic membrane which depolarizes and deenergizes the cell. The active channel-forming domain consists

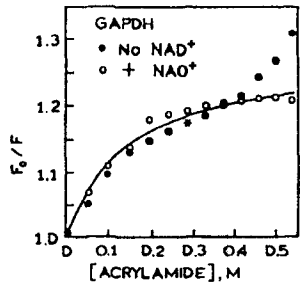

Figure 8.19. Acrylamide quenching of OAPDH in the absence (•) and in the presence (o) of the cofactor NAD^+. Revised from Ref. 47.

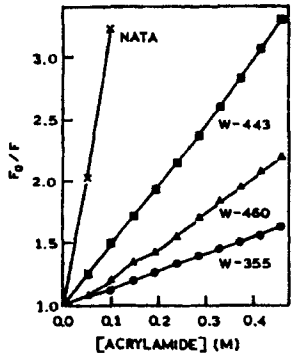

Figure 8.20. Stern–Volmer plots for acrylamide quenching of NATA (x) and three single-tryptophan mutants of the channel-forming peptide of colicin E1, W-355 (●), W-460 (▲), and W-443 (■). Revised from Ref. 48.

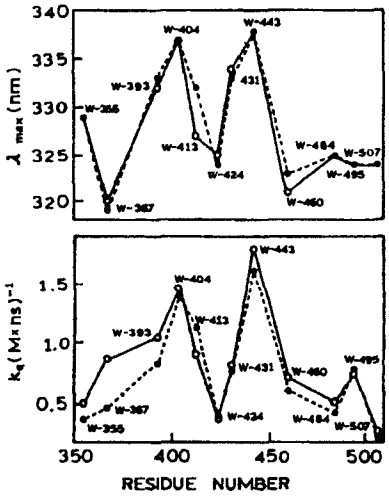

Figure 8.21. Emission maxima (*top*) and bimolecular quenching constants (*bottom*) of 12 single-tryptophan mutants of the channel-forming peptide of colicin E1. Revised and reprinted, with permission, from Ref. 48, Copyright © 1993, American Chemical Society.

of about 200 residues from the carboxy terminus, which form 10 α-helices spanning the membrane.

The conformation of the membrane-bound form of the colicin E1 channel peptide was studied by acrylamide quenching.[48] Twelve single-tryptophan mutants were formed by site-directed mutagenesis. The tryptophan residues were mostly conservative replacements, meaning that the trp residues were placed in positions previously containing phenylalanine or tyrosine. Stern–Volmer plots for acrylamide quenching of three of these mutant proteins and of NATA are shown in Figure 8.20. The accessibility to acrylamide quenching is strongly dependent on the location of the residue, and all residues are shielded relative to NATA. Depending on position, the trp residues also showed different emission maxima (Figure 8.21). The acrylamide bimolecular quenching constants were found to closely follow the emission maxima, with lower values of k_q for the shorter-wavelength tryptophans. Such data can be used to suggest a folding pattern for the channel-forming peptide and to reveal conformational changes that occur upon pH activation of colicin E1.

8.10. QUENCHING-RESOLVED EMISSION SPECTRA
• **Advanced Topic** •

8.10.A. Fluorophore Mixtures

As shown in Section 8.8, the emission spectra of proteins often shift in the presence of quenching. This effect occurs because the various trp residues are differently sensitive to quenching. Stated alternatively, for a mixture of fluorophores, quenching is expected to be dependent on the observation wavelength. This concept has been extended to calculation of the underlying emission spectra from the wavelength-dependent quenching data.[49–54] This is accomplished by measuring a Stern–Volmer plot for each emission wavelength (λ). For more than one fluorophore, the wavelength-dependent data can be described by

$$\frac{F(\lambda)}{F_0(\lambda)} = \sum_i \frac{f_i(\lambda)}{1 + K_i(\lambda)[Q]} \qquad [8.32]$$

where $f_i(\lambda)$ is the fractional contribution of the ith fluorophore to the steady-state intensity at wavelength λ, and $K_i(\lambda)$ is the Stern–Volmer quencher constant of the ith species at λ. For a single fluorophore, the quenching constant is usually independent of emission wavelength, i.e., $K_i(\lambda) = K_i$.

In order to resolve the individual emission spectra, the data are analyzed by nonlinear least-squares analysis.

Typically, one performs a global analysis in which the K_i values are global, and the $f_i(\lambda)$ values are variable at each wavelength. The result of the analysis is a set of K_i values, one for each component, and the fractional intensities $f_i(\lambda)$ at each wavelength, with $\Sigma f_i(\lambda) = 1.0$. The values of $f_i(\lambda)$ are used to calculate the emission spectrum of each component,

$$F_i(\lambda) = f_i(\lambda)F(\lambda) \qquad [8.33]$$

where $F(\lambda)$ is the steady-state emission spectrum of the sample.

The use of quenching-resolved spectra is illustrated by a sample containing both DPH and 5-((((2-iodoacetyl)amino)ethyl)amino)naphthalene-1-sulfonic acid (IAEDANS). These fluorophores were studied in SDS micelles, where their emission spectra are distinct (Figure 8.22). DPH is not soluble in water, so all the DPH is expected to be dissolved in the SDS micelles. IAEDANS is water-soluble and negatively charged, so it is not expected to bind to the negatively charged SDS micelles. Hence, IAEDANS is expected to be quenched by the water-soluble quencher acrylamide, and DPH is not expected to be accessible to acrylamide quenching.

Stern–Volmer plots for acrylamide quenching of the DPH–IAEDANS mixture as well as the individual fluorophores are shown in Figure 8.23. As predicted from the solubilities of the probes and acrylamide in water, DPH is weakly quenched by acrylamide. In contrast, IAEDANS is strongly quenched. The extent of quenching for the mixture is intermediate between that observed for each probe alone. As expected for a mixture of fluorophores, the

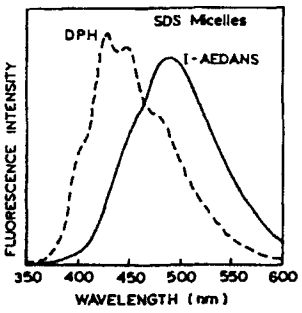

Figure 8.22. Steady-state emission spectra of DPH (—) and IAEDANS (—) in 1.2m*M* SDS micelles at 23 °C. The concentration of DPH was 2μ*M*, and that of IAEDANS was 170μ*M*. The excitation wavelength was 337 nm. Revised from Ref. 49.

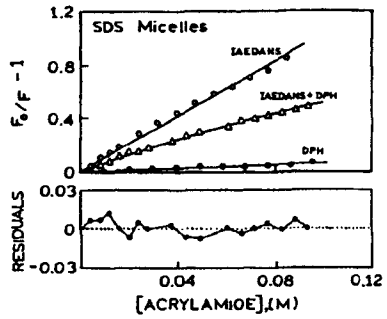

Figure 8.23. Stern–Volmer plots for acrylamide quenching of IAEDANS (○), DPH (●), and IAEDANS and DPH (△) in SDS micelles. For the mixture, the solid line represents the fit with calculated parameters $K_1 = 9.9\,M^{-1}$, $K_2 = 0\,M^{-1}$, $f_1 = 0.69$, and $f_2 = 0.31$ at 473 nm. The lower panel shows the residuals for this fit. Revised from Ref. 49.

Stern–Volmer plot curves downward due to the increasing fractional contribution of the more weakly quenched species at higher quencher concentrations.

The curvature in the Stern–Volmer plots was used to recover the values of $K_i(\lambda)$ and $f_i(\lambda)$ at each wavelength. In this case the $K_i(\lambda)$ values were not used as global parameters, so that $K_1(\lambda)$ and $K_2(\lambda)$ were obtained for each wavelength. At all wavelengths, there were two values near $0.5M^{-1}$ and $9.5M^{-1}$, representing the quenching constants of DPH and IAEDANS, respectively. At the shortest wavelength, below 420 nm, there is only one $K_i(\lambda)$ value because only DPH emits. The recovered values of $f_i(\lambda)$ were used to calculate the individual spectra from the spectrum of the mixture (Figure 8.24). In Chapters 4 and 5 we saw how the component spectra for heterogeneous samples could be resolved using the TD or the FD data. The use of wavelength-dependent quenching provides similar results, without the use of complex instrumentation. Of course, the method depends on the probes being differently sensitive to collisional quenching, which normally occurs if the decay times are different.

8.10.B. Quenching-Resolved Emission Spectra of the *E. coli* Tet Repressor

The Tet repressor from *E. coli* is a DNA-binding protein which controls the expression of genes that confer resistance to tetracycline. This protein contains two tryptophan residues at positions 43 and 75. W43 is thought to be an exposed residue, and W75 is thought to be buried in the protein matrix.[54] Earlier studies of single-tryptophan mu-

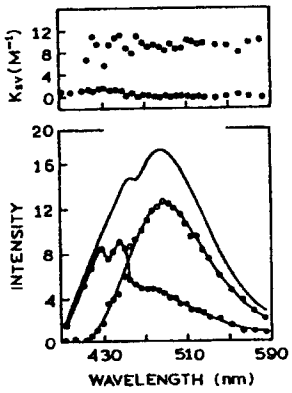

Figure 8.24. *Bottom:* Emission spectrum of the DPH-IAEDANS mixture and quenching-resolved emission spectra of DPH (●) and IAEDANS (○). *Top:* Wavelength dependence of the quenching constants, with average values of $K_1 = 9.6\ M^{-1}$ and $K_2 = 0.47\ M^{-1}$. Revised from Ref. 49.

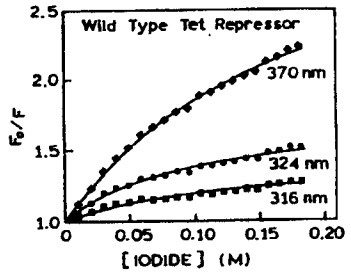

Figure 8.25. Stern–Volmer iodide plots for iodide quenching of the wild-type Tet repressor. The emission wavelengths are indicated on the figure. The solution contained 1 m*M* sodium thiosulfate to prevent formation of I_3^-. From Ref. 54.

tants of the Tet repressor confirmed the accessibility of W43 to iodide and the shielding of W75 from iodide quenching.[55] Hence, this protein provided an ideal model protein with which to attempt quenching resolution of the individual emission spectra of two tryptophan residues in a protein.

Stern–Volmer plots for iodide quenching of the Tet repressor were measured for various emission wavelengths[54] (Figure 8.25). A larger amount of quenching was observed for longer wavelengths. When the quenching data were analyzed in terms of two components, one of these components was found to be almost inaccessible to iodide. For instance, at 324 nm the recovered values are $f_1 = 0.34$, $K_1 = 16.2\ M^{-1}$, $f_2 = 0.66$, and $K_2 = 0$. The wavelength-dependent data were used to calculate the individual spectra (Figure 8.26). The blue-shifted spectrum with a maximum at 324 nm corresponds to the inaccessible fraction, and the red-shifted spectrum with a maximum at 349 nm is the fraction accessible to iodide quenching. These emission spectra are assigned to W-75 and W-43, respectively.

The results in the top panel of Figure 8.26 illustrate one difficulty often encountered in the determination of quenching-resolved spectra. The quenching constant for a single species can be dependent on emission wavelength. In this case the quenching constant of the accessible tryptophan changed about twofold across its emission spectrum. When this occurs, the values of $K_i(\lambda)$ cannot be treated as global parameters.

The assignments of the quenching-resolved spectra are consistent with the results obtained using single-tryptophan mutants of the Tet repressor[55] (Figure 8.27). Little, if any, quenching was observed for the protein containing only W-75, and W-43 was readily quenched by iodide. Iodide quenching of the wild-type protein is intermediate between that of the two single-tryptophan mutants. While

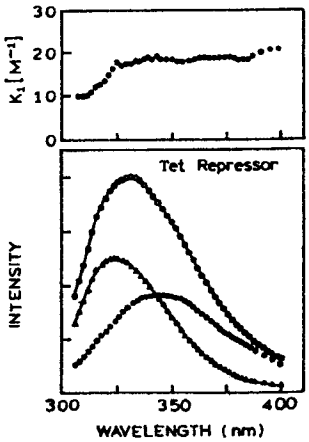

Figure 8.26. *Bottom:* Fluorescence quenching-resolved spectra of wild-type Tet repressor, obtained using potassium iodide as the quencher. *Top:* Wavelength-dependent values of K_1. From Ref. 54.

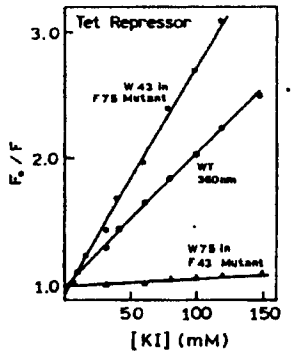

Figure 8.27. Stern–Volmer plots for the iodide quenching of *E. coli* Tet repressor (wild type, WT) and its mutants (F43 and F75). Revised from Ref. 55.

the same information is available from the mutant proteins, the use of quenching provided the resolved spectra with the use of only the wild-type protein.

It is valuable to notice a difference in the method of data analysis for the modified Stern–Volmer plots (Section 8.8.A) and for the quenching-resolved emission spectra. In analyzing a modified Stern–Volmer plot, one assumes that a fraction of the fluorescence is totally inaccessible to quenchers. This may not be completely true because one component can be more weakly quenched, but still quenched to some extent. If possible, it is preferable to analyze the Stern–Volmer plots by nonlinear least-squares analysis when the f_i and K_i values are variable. With this approach, one allows each component to contribute to the data according to its fractional accessibility, instead of forcing one component to be an inaccessible fraction. Of course, such an analysis is more complex, and the data may not be adequate to recover the values of f_i and K_i at each wavelength.

8.11. QUENCHING AND ASSOCIATION REACTIONS

8.11.A. Quenching Due to Specific Binding Interactions

In the preceding sections we considered quenchers that were in solution with the macromolecule but did not display any specific interactions. Such interactions can occur and can appear to be of static quenching.[56–59] One example is provided by serum albumin. Serum albumin consists of a single polypeptide chain, with a molecular weight near 65,000. Albumin is present in high concentrations in blood serum, 35–45 mg/ml, and is important for maintaining osmotic balance and for transport of hydrophobic species. Albumins have hydrophobic sites which are known to bind fatty acids and many fluorescent probes. Human serum albumin (HSA) has a single tryptophan residue, and bovine serum albumin (BSA) has two tryptophan residues.

BSA and HSA can bind halogenated anesthetics. This binding is seen by the effect of chloroform ($CHCl_3$) on the fluorescence intensity of BSA (Figure 8.28). Addition of $CHCl_3$ is seen to result in a progressive decrease in the fluorescence intensity of BSA. In the paper in which these results were reported,[58] there was no mention of photochemical effects, which we found surprising; in our experience, excitation of tryptophan in the presence of $CHCl_3$ results in the formation of blue fluorescent species.

The dependence of the BSA emission on the $CHCl_3$ concentration is shown in Figure 8.29 along with the effects of $CHCl_3$ on the emission of tryptophan and another protein, apomyoglobin. The effect of $CHCl_3$ on BSA is greater than that seen for trp or apomyoglobin, suggesting a specific interaction with BSA. The fact that there is hydrophobic binding of $CHCl_3$ to BSA is shown by the effect of trifluoroethanol (TFE), which disrupts hydrophobic binding. In 50% TFE, $CHCl_3$ no longer quenches BSA to the extent seen in water.

How can one determine whether the quenching seen for BSA in water is due to $CHCl_3$ binding or to collisional quenching? One method is to calculate the apparent bimolecular quenching constant (k_q^{app}). Assume that the decay time of BSA is near 5 ns. The data in Figure 8.29 indicate a K_{SV} value of 400 M^{-1}. The fluorescence is 50% quenched at 2.5mM $CHCl_3$. These values correspond to a bimolecular quenching constant of $k_q^{app} = 8 \times 10^{10}\ M^{-1}\ s^{-1}$, which is about 10-fold larger than the maximum value possible for diffusion-limited quenching

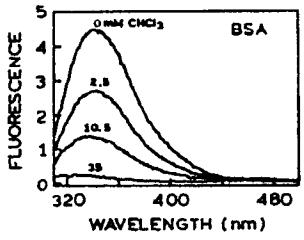

Figure 8.28. Emission spectra of BSA in the presence of various concentrations of chloroform. Revised from Ref. 58.

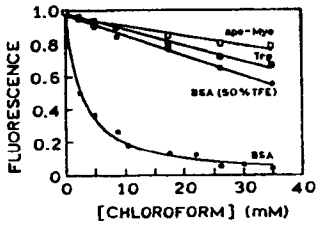

Figure 8.29. Fluorescence intensities of BSA (●), tryptophan (■), and apomyoglobin (□) in the presence of various amounts of dissolved $CHCl_3$. O, BSA in 50% trifluoroethanol (TFE), which disrupts hydrophobic binding to BSA. Revised from Ref. 58.

in water. Hence, there must be some interaction that increases the local concentrations of $CHCl_3$ around the trp residues in BSA. Since there is no reason to expect ground-state complex formation between trp and $CHCl_3$, the quenching may be dynamic. However, the $CHCl_3$ is probably bound in close proximity to the trp residues, giving the appearance of a dark complex.

Another example of quenching due to a specific binding interaction is shown in Figure 8.30 for binding of caffeine to HSA, an experiment most of us start each morning. The Stern–Volmer plots show a value of $K_{SV} \simeq 7150\ M^{-1}$. This value is obviously too large to be due to collisional quenching, especially for a lifetime near 5 ns. The value of k_q^{app} is $1.4 \times 10^{12}\ s^{-1}$, over 100-fold larger than the maximum diffusion-limited rate. Hence, the caffeine must be bound to the HSA. Caffeine is an electron-deficient molecule and may form ground-state complexes with indole. This possibility could be tested by examination of the absorption spectra of HSA in the absence and presence of caffeine. If ground-state association with indole occurs, then the trp absorption spectrum is expected to change. Another indicator of complex formation is the temperature dependence

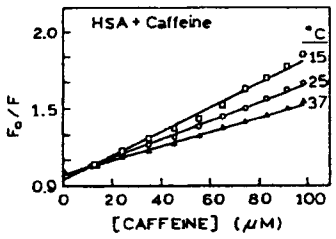

Figure 8.30. Quenching of HSA by caffeine at three temperatures. Revised from Ref. 59.

of the Stern–Volmer plots. For diffusive quenching, one expects more quenching at higher temperatures. In the case of HSA and caffeine, there is less quenching at higher temperatures (Figure 8.30), which suggests that the complex is less stable at higher temperatures.

8.11.B. Binding of Substrates to Ribozymes

The catalytic properties of highly structured RNAs have been the subject of numerous studies since 1982, when it was first reported that certain RNAs, termed ribozymes, could display enzymatic activity. One example is the hairpin ribozyme, which cleaves single-stranded RNA (Figure 8.31). The early observations of quenching by nucleotides[17,18] (Section 8.5) provided the opportunity to study substrate binding to ribozymes. The substrate contained a fluorescein residue covalently linked at the 3′-end. The hairpin ribozyme contains a guanosine residue at the 5′-end. Upon binding of substrate nucleotide to the ribozyme, the fluorescein emission is quenched (Figure 8.32). Quenching also occurs when the fluorescein-labeled substrate binds to the substrate-binding strand (SBS) which contains a 5′-guanosine residue (G-SBS). The guanosine residue is needed for quenching, and the emission of fluorescein is unchanged in the presence of the substrate-binding strand without a 5′-terminal guanosine residue (not shown in Figure 8.32). This example shows how

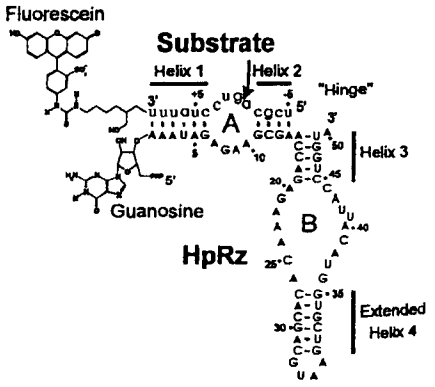

Figure 8.31. Structure of the hairpin ribozyme (HpRz) and the fluorescein-labeled substrate. The substrate-binding strand is the region adjacent to the substrate. Reprinted, with permission, from Ref. 60, Copyright © 1997, Cambridge University Press.

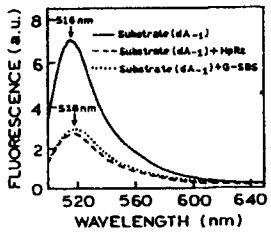

Figure 8.32. Emission spectra of the fluorescein-labeled substrate analog (dA_{-1}) in solution and when bound to the hairpin ribozyme (HpRz) or the guanosine-containing substrate-binding strand (G-SBS). From Ref. 60.

fundamental studies of nucleotide quenching have found useful applications in modern biochemistry.

8.11.C. Association Reactions and Quenching

Fluorescence is often used to measure association reactions. This requires that the fluorescence of one of the reactants changes upon binding. While this often occurs, it is not always the case. One example is the binding of ε-ADP to the DnaB helicase hexamer. The fluorescence of ε-ADP displayed only a small increase upon binding to the protein. Collisional quenching was used to induce a larger change in fluorescence on binding.[61] Acrylamide is an efficient quencher of ε-ADP, which should be quenched more strongly in solution than when bound to the helicase. Hence, if the binding is studied in a solution which contains acrylamide, there should be an increase in ε-ADP fluorescence on binding to the helicase.

Solutions of ε-ADP were titrated with the helicase (Figure 8.33). In the absence of acrylamide, there was little change in the ε-ADP fluorescence. The titrations were performed again, in solutions with increasing amounts of acrylamide. Under these conditions, ε-ADP showed an increase in fluorescence upon binding. This increase occurred because the ε-ADP became shielded from acrylamide upon binding to helicase. The authors also showed that acrylamide had no effect on the affinity of ε-ADP for helicase.[61] In this system the use of a quencher allowed measurement of a binding reaction that would otherwise be difficult to measure.

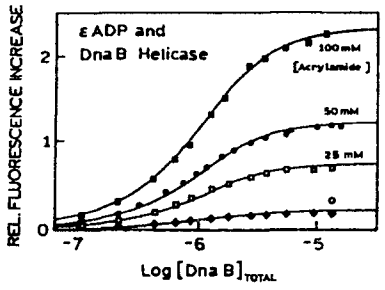

Figure 8.33. Fluorescence titration of ε-ADP, at a constant concentration of nucleotide, with the DnaB helicase in buffer containing different concentrations of acrylamide. Revised and reprinted from Ref. 61, Copyright © 1997, with permission from Elsevier Science.

8.12. INTRAMOLECULAR QUENCHING

Quenching can also occur between covalently linked fluorophore–quencher pairs.[62,63] One common example is the formation of exciplexes by covalently linked aromatic hydrocarbons and amines.[64,65] Another example is the covalent adduct formation by indole and acrylamide. For example, the lifetime of *N*-acetyltryptamine is near 5.1 ns. When the acetyl group is replaced by an acryloyl group, the lifetime is reduced to 31 ps (Figure 8.34). Similarly, covalent attachment of spin labels to a naphthalene derivative reduced its lifetime from 33.7 to 1.1 ns.

The concept of intramolecular quenching can be used to obtain structural information[66] as was demonstrated for a

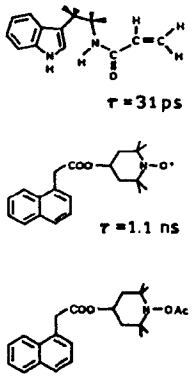

Figure 8.34. Fluorophore–quencher conjugates which display intramolecular quenching.[62,63]

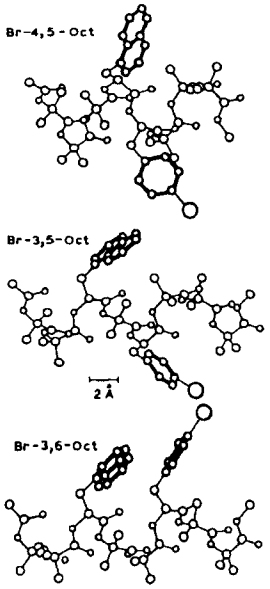

Figure 8.35. Structure of peptides containing naphthylalanine and *p*-bromophenylalanine, separated by 0 (*top*), 1 (*middle*), or 2 (*bottom*) amino acid residues. Revised and reprinted, with permission, from Ref. 66, Copyright © 1993, American Chemical Society.

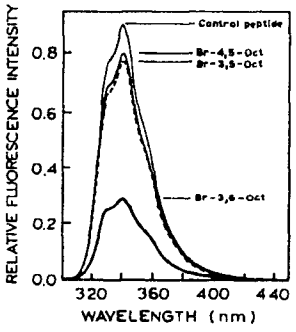

Figure 8.36. Emission spectra of the peptides shown in Figure 8.45. Also shown is the emission spectrum of a control peptide with a phenylalanine group in place of *p*-bromophenylalanine. Revised and reprinted, with permission, from Ref. 66, Copyright © 1993, American Chemical Society.

series of peptides containing a naphthylalanine fluorophore and a *p*-bromophenylalanine quencher (Figure 8.35). The probe and quencher were separated by 0, 1, or 2 amino acid residues. Emission spectra of these peptides show minimal quenching except for separation by 2 amino acid residues (Figure 8.36). In this case the fluorophore and quencher are adjacent, resulting in over 50% quenching of the naphthylalanine. These results suggest that, in solution, this peptide adopts a conformation with the bromo group near the indole ring.

8.13. QUENCHING OF PHOSPHORESCENCE

Phosphorescence is not usually observed in fluid solutions near room temperature. One reason for the absence of phosphorescence is the long phosphorescence lifetimes and the presence of dissolved oxygen and other quenchers. For instance, recent data for tryptophan revealed a phosphorescence lifetime of 1.2 ms at 20 °C.[67] Suppose that the oxygen bimolecular quenching constant is $1 \times 10^{10} M^{-1}\,s^{-1}$ and that the aqueous sample is in equilibrium with dissolved oxygen from the air (0.255mM O_2). Using Eq. [8.1], the intensity is expected to be quenched 3000-fold. For this reason, methods have been developed to remove dissolved oxygen from samples used to study phosphorescence.[68,69] In practice, other dissolved quenchers and nonradiative decay rates result in vanishingly small phosphorescence quantum yields in room-temperature solutions. Some exceptions are known, such as when fluorophores are located in highly protected environments within proteins.[70-73] Phosphorescence has also been observed at room temperature for probes bound to cyclodextrins, even in the pres-

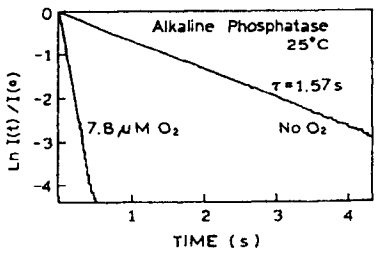

Figure 8.37. Phosphorescence decay of alkaline phosphatase at 25 °C in the absence of oxygen and in the presence of 7.8μM oxygen. Revised and reprinted, with permission, from Ref. 77, Copyright © 1987, Biophysical Society.

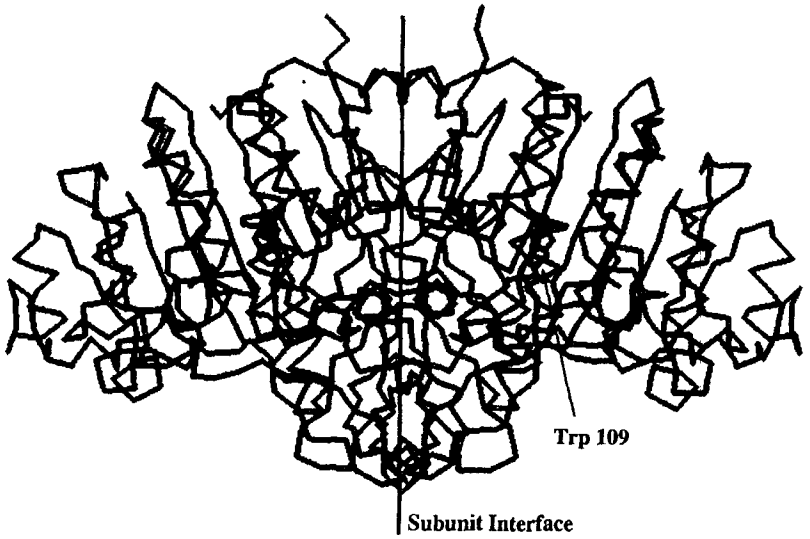

Figure 8.38. Structure of the alkaline phosphatase dimer, showing the phosphorescent residue trp-109. Courtesy of Dr. Ari Gafni, University of Michigan.

ence of oxygen.[74] However, in general, phosphorescence is not commonly observed near room temperature.

Protein phosphorescence can be quenched by a number of small molecules such as amino acids, H_2O, and CS_2,[75,76] in addition to oxygen. An example of the dramatic quenching of protein phosphorescence by even low concentrations of oxygen is shown for alkaline phosphatase phosphorescence[77] in Figure 8.37. It is now known that the phosphorescence from alkaline phosphatase results from one of its three nonidentical tryptophan residues, trp-109. This residue is located in a highly shielded environment near the dimer interface (Figure 8.38). In the presence of $7.8\mu M$ oxygen, the phosphorescence lifetime is reduced from 1.57 s to 0.1 s. Note that an oxygen concentration of $7.8\mu M$ would have an insignificant effect on nanosecond fluorescence. It is also important to notice that trp-109 in alkaline phosphatase is one of the most shielded residues identified to date in a protein. The lifetimes in the absence and presence of $7.8\mu M$ oxygen can be used to calculate a value of $1.2 \times 10^6\ M^{-1}\ s^{-1}$ for the bimolecular quenching constant k_q. If the residue were more typical, with a k_q value of $0.1 \times 10^9\ M^{-1}\ s^{-1}$, one can calculate that the decay time in $7.8\mu M$ oxygen would have been reduced to 1.28 ms, and thus quenched by over 1000-fold for a micromolar quencher concentration.

REFERENCES

1. Kautsky, H., 1939, Quenching of luminescence by oxygen, *Trans. Faraday Soc.* 35:216–219.
2. Knibbe, H., Rehm, D., and Weller, A., 1968, Intermediates and kinetics of fluorescence quenching by electron transfer, *Ber. Bunsenges. Phys. Chem.* 72:257–263.
3. Kasha, M., 1952, Collisional perturbation of spin–orbital coupling and the mechanism of fluorescence quenching. A visual demonstration of the perturbation, *J. Chem. Phys.* 20:71–74.
4. Steiner, R. F., and Kirby, E. P., 1969, The interaction of the ground and excited states of indole derivatives with electron scavengers, *J. Phys. Chem.* 73:4130–4135.
5. Eftink, M. R., and Ghiron, C., 1981, Fluorescence quenching studies with proteins, *Anal. Biochem.* 114:199–227.
6. Eftink, M. R., 1991, Fluorescence quenching reactions: Probing biological macromolecular structures, in *Biophysical and Biochemical Aspects of Fluorescence Spectroscopy*, T. G. Dewey (ed.), Plenum Press, New York, pp. 1–41.
7. Eftink, M. R., 1991, Fluorescence quenching: Theory and applications, in *Topics in Fluorescence Spectroscopy, Volume 2, Principles*, J. R. Lakowicz (ed.), Plenum Press, New York, pp. 53–126.

8. Davis, G. A., 1973, Quenching of aromatic hydrocarbons by alkylpyridinium halides, *J. Chem. Soc., Chem. Commun.* 1973:728–729.
9. Shinitzky, M., and Rivnay, B., 1977, Degree of exposure of membrane proteins determined by fluorescence quenching, *Biochemistry* 16:982–986.
10. Spencer, R. D., and Weber, G., 1972, Thermodynamics and kinetics of the intramolecular complex in flavin-adenine dinucleotide, in *Structure and Function of Oxidation Reduction Enzymes*, A. Akeson and A. Ehrenberg (eds.), Pergamon Press, New York, pp. 393–399.
11. Scott, T. G., Spencer, R. D., Leonard, N. J., and Weber, G., 1970, Emission properties of NADH. Studies of fluorescence lifetimes and quantum efficiencies of NADH, AcPyADH, and simplified synthetic models, *J. Am. Chem. Soc.* 92:687–695.
12. Ware, W. R., 1962, Oxygen quenching of fluorescence in solution: An experimental study of the diffusion process, *J. Phys. Chem.* 66:455–458.
13. Othmer, D. F., and Thakar, M. S., 1953, Correlating diffusion coefficients in liquids, *Ind. Eng. Chem.* 45:589–593.
14. Lakowicz, J. R., and Weber, G., 1973, Quenching of fluorescence by oxygen. A probe for structural fluctuations in macromolecules, *Biochemistry* 12:4161–4170.
15. Eftink, M. R., and Ghiron, C. A., 1976, Fluorescence quenching of indole and model micelle systems, *J. Phys. Chem.* 80:486–493.
16. Johnson, D. A., and Yguerabide, J., 1985, Solute accessibility to *N'*-fluorescein isothiocyanate-lysine-23, cobra α-toxin bound to the acetylcholine receptor, *Biophys. J.* 48:949–955.
17. Kubota, Y., Nakamura, H., Morishita, M., and Fujisaki, Y., 1978, Interaction of 9-aminoacridine with 7-methylguanosine and $1,N^6$-ethenoadenosine monophosphate, *Photochem. Photobiol.* 27:479–481.
18. Kubota, Y., Motoda, Y., Shigemune, Y., and Fujisaki, Y., 1979, Fluorescence quenching of 10-methylacridinium chloride by nucleotides, *Photochem. Photobiol.* 29:1099–1106.
19. Seidel, C. A. M., Schulz, A., and Sauer, M. H. M., 1996, Nucleobase-specific quenching of fluorescent dyes. 1. Nucleobase one-electron redox potentials and their correlation with static and dynamic quenching efficiencies, *J. Phys. Chem.* 100:5541–5553.
20. Casali, E., Petra, P. H., and Ross, J. B. A., 1990, Fluorescence investigation of the sex steroid binding protein of rabbit serum: Steroid binding and subunit dissociation, *Biochemistry* 29:9334–9343.
21. Frank, I. M., and Vavilov, S. I., 1931, Über die wirkungssphäre der auslöschungs-vargänge in den flureszierenden flussigHeiten. *Z. Phys.* 69:100–110.
22. Maniara, G., Vanderkooi, J. M., Bloomgarden, D. C., and Kolóczek, H., 1988, Phosphorescence from 2-(*p*-toluidinyl)naphthalene-6-sulfonate and 1-anilinonaphthalene-8-sulfonate, commonly used fluorescence probes of biological structures, *Photochem. Photobiol.* 47:207–208.
23. Kim, H., Crouch, S. R., and Zabik, M. J., 1989, Room-temperature phosphorescence of compounds in mixed organized media: Synthetic enzyme model-surfactant system, *Anal. Chem.* 61:2475–2478.
24. Encinas, M. V., Lissi, E. A., and Rufs, A. M., 1993, Inclusion and fluorescence quenching of 2,3-dimethylnaphthalene in β-cyclodextrin cavities, *Photochem. Photobiol.* 57:603–608.
25. Turro, N. J., Bolt, J. D., Kuroda, Y., and Tabushi, I., 1982, A study of the kinetics of inclusion of haloaphthalenes with β-cyclodextrin via time correlated phosphorescence, *Photochem. Photobiol.* 35:69–72.
26. Waka, Y., Hamamoto, K., and Mataga, N., 1980, Heteroexcimer systems in aqueous micellar solutions, *Photochem. Photobiol.* 32:27–35.
27. Atherton, S. J., and Beaumont, P. C., 1986, Quenching of the fluorescence of DNA-intercalated ethidium bromide by some transition metal ions, *J. Phys. Chem.* 90:2252–2259.
28. Pasternack, R. F., Caccam, M., Keogh, B., Stephenson, T. A., Williams, A. P., and Gibbs, E. J., 1991, Long-range fluorescence quenching of ethidium ion by cationic porphyrins in the presence of DNA, *J. Am. Chem. Soc.* 113:6835–6840.
29. Poulos, A. T., Kuzmin, V., and Geacintov, N. E., 1982, Probing the microenvironment of benzo[*a*]pyrene diol epoxide–DNA adducts by triplet excited state quenching methods, *J. Biochem. Biophys. Methods* 6:269–281.
30. Zinger, D., and Geacintov, N. E., 1988, Acrylamide and molecular oxygen fluorescence quenching as a probe of solvent-accessibility of aromatic fluorophores complexed with DNA in relation to their conformations: Coronene-DNA and other complexes, *Photochem. Photobiol.* 47:181–188.
31. Suh, D., and Chaires, J. B., 1995, Criteria for the mode of binding of DNA binding agents, *Bioorgan. Med. Chem.* 3:723–728.
32. Ando, T., and Asai, H., 1980, Charge effects on the dynamic quenching of fluorescence of $1,N^6$-ethenoadenosine oligophosphates by iodide, thallium (I) and acrylamide, *J. Biochem.* 88:255–264.
33. Ando, T., Fujisaki, H., and Asai, H., 1980, Electric potential at regions near the two specific thiols of heavy meromyosin determined by the fluorescence quenching technique, *J. Biochem.* 88:265–276.
34. Miyata, H., and Asai, H., 1981, Amphoteric charge distribution at the enzymatic site of $1,N^6$-ethenoadenosine triphosphate-binding heavy meromyosin determined by dynamic fluorescence quenching, *J. Biochem.* 90:133–139.
35. Midoux, P., Wahl, P., Auchet, J.-C., and Monsigny, M., 1984, Fluorescence quenching of tryptophan by trifluoroacetamide, *Biochim. Biophys. Acta* 801:16–25.
36. Lehrer, S. S., 1971, Solute perturbation of protein fluorescence. The quenching of the tryptophan fluorescence of model compounds and of lysozyme by iodide ion, *Biochemistry* 10:3254–3263.
37. Eftink, M. R., and Selvidge, L. A., 1982, Fluorescence quenching of liver alcohol dehydrogenase by acrylamide, *Biochemistry* 21:117–125.
38. Eftink, M., and Haganman, K. A., 1986, Fluorescence lifetime and anisotropy studies with liver alcohol dehydrogenase and its complexes, *Biochemistry* 25:6631–6637.
39. Sontag, B., Reboud, A.-M., Divita, G., Di Pietro, A., Guillot, D., and Reboud, J.P., 1993, Intrinsic tryptophan fluorescence of rat liver elongation factor eEF-2 to monitor the interaction with guanylic and adenylic nucleotides and related conformational changes, *Biochemistry* 32:1976–1980.
40. Xing, D., Dorr, R., Cunningham, R. P., and Scholes, C. P., 1995, Endonuclease III interactions with DNA substrates. 2. The DNA repair enzyme endonuclease III binds differently to intact DNA and to apyrimidinic/aprinic DNA substrates as shown by tryptophan fluorescence quenching, *Biochemistry* 34:2537–2544.
41. Wasylewski, M., Malecki, J., and Wasylewski, Z., 1995, Fluorescence study of *Escherichia coli* cyclic AMP receptor protein, *J. Protein Chem.* 14:299–308.
42. Wells, T. A., Nakazawa, M., Masuhe, K., and Song, P.-S., 1994, A conformational change associated with the phototransformation of *Pisum* phytochrome A as probed by fluorescence quenching, *Biochemistry* 33:708–712.

43. Eftink, M. R., Zajicek, J. L., and Ghiron, C. A., 1977, A hydrophobic quencher of protein fluorescence: 2,2,2-Trichloroethanol, *Biochim. Biophys. Acta* **491**:473–481.
44. Blatt, E., Husain, A., and Sawyer, W. H., 1986, The association of acrylamide with proteins. The interpretation of fluorescence quenching experiments, *Biochim. Biophys. Acta* **871**:6–13.
45. Eftink, M. R., and Ghiron, C. A., 1987, Does the fluorescence quencher acrylamide bind to proteins? *Biochim. Biophys. Acta* **916**:343–349.
46. Punyiczki, M., Norman, J. A., and Rosenberg, A., 1993, Interaction of acrylamide with proteins in the concentration range used for fluorescence quenching studies, *Biophys. Chem.* **47**:9–19.
47. Bastyns, K., and Engelborghs, Y., 1992, Acrylamide quenching of the fluorescence of glyceraldehyde-3-phosphate dehydrogenase: Reversible and irreversible effects, *Photochem. Photobiol.* **55**:9–16.
48. Merrill, A. R., Palmer, L. R., and Szabo, A. G., 1993, Acrylamide quenching of the intrinsic fluorescence of tryptophan residues genetically engineered into the soluble colicin E1 channel peptide. Structural characterization of the insertion-competent state, *Biochemistry* **32**:6974–6981.
49. Wasylewski, Z., Kaszycki, P., Guz, A., and Stryjewski, W., 1988, Fluorescence quenching resolved spectra of fluorophores in mixtures and micellar solutions, *Eur. J. Biochem.* **178**:471–476.
50. Wasylewski, Z., Kolodziek, H., and Wasniowska, A., 1988, Fluorescence quenching resolved spectroscopy of proteins, *Eur. J. Biochem.* **172**:719–724.
51. Laws, W. R., and Shore, J. D., 1978, The mechanism of quenching of liver alcohol dehydrogenase fluorescence due to ternary complex formation, *J. Biol. Chem.* **23**:8593–8597.
52. Stryjewski, W., and Wasylewski, Z., 1986, The resolution of heterogeneous fluorescence of multityrptophan-containing proteins studied by a fluorescence quenching method, *Eur. J. Biochem.* **158**:547–553.
53. Blicharska, Z., and Wasylewski, Z., 1995, Fluorescence quenching studies of trp repressor using single-tryptophan mutants, *J. Protein Chem.* **14**:739–746.
54. Wasylewski, Z., Kaszycki, P., and Drwiega, M., 1996, A fluorescence study of Tn10-encoded tet repressor, *J. Protein Chem.* **15**:45–52.
55. Hansen, D., Altschmied, L., and Hillen, W., 1987, Engineered tet repressor mutants with single tryptophan residues as fluorescent probes, *J. Biol. Chem.* **29**:14030–14035.
56. Lange, R., Amrenbacher, P., Müller, S., Maurin, L., and Balny, C., 1994, Interaction of tryptophan residues of cytochrome P45scc with a highly specific fluorescence quencher, a substrate analogue, compared to acrylamide and iodide, *Eur. J. Biochem.* **226**:963–970.
57. Johansson, J. S., Eckenhoff, R. G., and Dutton, L., 1995, Binding of halothane to serum albumin demonstrated using tryptophan fluorescence, *Anesthesiology* **83**:316–324.
58. Johansson, J. S., 1997, Binding of the volatile anesthetic chloroform to albumin demonstrated using tryptophan fluorescence quenching, *J. Biol. Chem.* **272**:17961–17965.
59. Gonzalez-Jimenez, J., Frutos, G., and Cayre, I., 1992, Fluorescence quenching of human serum albumin by xanthines, *Biochem. Pharmacol.* **44**:824–826.
60. Walter, N. O., and Burke, J. M., 1997, Real-time monitoring of hairpin ribozyme kinetics through base-specific quenching of fluorescein-labeled substrates, *RNA* **3**:392–404.
61. Jezewska, M. J., and Bujalowski, W., 1997, Quantitative analysis of ligand–macromolecule interactions using differential dynamic quenching of the ligand fluorescence to monitor the binding, *Biophys. Chem.* **64**:253–269.
62. Eftink, M. R., Jia, Y.-W., Graves, D. E., Wiczk, W., Gryczynski, I., and Lakowicz, J. R., 1989, Intramolecular fluorescence quenching in covalent acrylamide–indole adducts, *Photochem. Photobiol.* **49**:725–729.
63. Greca, S. A., Simpson, D. J., Zhou, G., Ho, P. S., and Blough, N. V., 1990, Intramolecular quenching of excited singlet states by stable nitroxyl radicals, *J. Am. Chem. Soc.* **112**:7337–7346.
64. Chuang, T. J., Cox, R. J., and Eisenthal, K. B., 1974, Picosecond studies of the excited charge-transfer interactions in anthracene-$(CH_2)_3$-*N*,*N*-dimethylaniline systems, *J. Am. Chem. Soc.* **96**:6828–6831.
65. Migita, M., Okada, T., Mataga, N., Sakata, Y., Misumi, S., Nakashima, N., and Yoshihara, K., 1981, Picosecond laser spectroscopy of intramolecular heteroexcimer systems. Time-resolved fluorescence studies of p-$(CH_3)_2NC_6H_4$-$(CH_2)_n$-(9-anthryl), p-$(CH_3)_2NC_6H_4$-$(CH_2)_n$-(1-pyrenyl) systems and 9,9′-bianthryl, *Bull. Chem. Soc. Jpn.* **54**:3304–3311.
66. Basu, G., Anglos, D., and Kuki, A., 1993, Fluorescence quenching in a strongly helical peptide series: The role of noncovalent pathways in modulating electronic interactions, *Biochemistry* **32**:3067–3076.
67. Strambini, G. B., and Gonnelli, M., 1995, Tryptophan phosphorescence in fluid solution, *J. Am. Chem. Soc.* **117**:7646–7651.
68. Englander, S. W., Calhoun, D. B., and Englander, J. J., 1987, Biochemistry without oxygen, *Anal. Biochem.* **161**:300–306.
69. Zhang, H. R., Zhang, J., Wei, Y. S., Jin, E. J., and Liu, C. S., 1997, Study of new facile deoxygenation methods in cyclodextrin induced room temperature phosphorescence, *Anal. Chim. Acta* **357**:119–125.
70. Cioni, P., Puntoni, A., and Strambini, G. B., 1993, Tryptophan phosphorescence as a monitor of the solution structure of phosphoglycerate kinase from yeast, *Biophys. Chem.* **46**:47–55.
71. Gonnelli, M., and Strambini, G. B., 1993, Glycerol effects on protein flexibility: A tryptophan phosphorescence study, *Biophys. J.* **65**:131–137.
72. Strambini, G. B., and Gabellieri, E., 1996, Proteins in frozen solutions: Evidence of ice-induced partial unfolding, *Biophys. J.* **70**:971–976.
73. Vanderkooi, J. M., Calhoun, D. B., and Englander, S. W., 1987, On the prevalence of room-temperature protein phosphorescence, *Science* **236**:568–569.
74. Turro, N. J., Cox, G. S., and Li, X., 1983, Remarkable inhibition of oxygen quenching of phosphorescence by complexation with cyclodextrins, *Photochem. Photobiol.* **37**:149–153.
75. Gonnelli, M., and Strambini, G. B., 1995, Phosphorescence lifetime of tryptophan in proteins, *Biochemistry* **34**:13847–13857.
76. Wright, W. W., Owen, C. S., and Vanderkooi, J. M., 1992, Penetration of analogues of H_2O and CO_2 in proteins studied by room temperature phosphorescence of tryptophan, *Biochemistry* **31**:6538–6544.
77. Strambini, G. B., 1987, Quenching of alkaline phosphatase phosphorescence by O_2 and NO, *Biophys. J.* **52**:23–28.
78. Boaz, H., and Rollefson, O. K., 1950, The quenching of fluorescence. Deviations from the Stern–Volmer law, *J. Am. Chem. Soc.* **72**:3425–3443.
79. Eftink, M. R., and Ghiron, C. A., 1976, Exposure of tryptophanyl residues in proteins. Quantitative determination by fluorescence quenching studies, *Biochemistry* **15**:672–680.
80. Kuzmin, M. O., and Gusova, L. N., 1969, Donor–acceptor complexes of singlet excited states of aromatic hydrocarbons with aliphatic amines, *Chem. Phys. Lett.* **3**:71–72.
81. Rehm, D., and Weller, A., 1970, Kinetics of fluorescence quenching by electron and H-atom transfer, *Israel J. Chem.* **8**:259–271.

82. Obytnovennaya, I. E., Vasileva, I. M., and Cherkasov, A. S., 1986, Quenching of the fluorescence of anthracene by dimethylaniline in aqueous-micellar solvent and formation of luminescent exciplexes, *Opt. Spectrosc.* **60**:169–171.
83. Lewis, F. D., and Bassani, D. M., 1992, Formation and decay of styrene–amine exciplexes, *J. Photochem. Photobiol. A: Chem.* **66**:43–52.
84. Schneider, S., Stammler, W., Bierl, R., and Jager, W., 1994, Ultrafast photoinduced charge separation and recombination in weakly bound complexes between oxazine dyes and *N,N*-dimethylaniline, *Chem. Phys. Lett.* **219**:433–439.
85. Yoshihara, K., Yartsev, A., Nagasawa, Y., Kandori, H., Douhal, A., and Kennitz, K., 1993, Femtosecond intermolecular electron transfer between dyes and electron-donating solvents, *Pure Appl. Chem.* **65**:1671–1675.
86. Bisht, P. B., and Tripathi, H. B., 1993, Fluorescence quenching of carbazole by triethylamine: Exciplex formation in polar and non-polar solvents, *J. Lumin.* **55**:153–158.
87. Sikaris, K. A., and Sawyer, W. H., 1982, The interaction of local anaesthetics with synthetic phospholipid bilayers, *Biochem. Pharmacol.* **31**:2625–2631.
88. Fernandez, M. S., and Calderon, E., 1990, The local anaesthetic tetracaine as a quencher of perylene fluorescence in micelles, *J. Photochem. Photobiol. B: Biol.* **7**:75–86.
89. Winkler, M. H., 1969, A fluorescence quenching technique for the investigation of the configurations of binding sites for small molecules, *Biochemistry* **8**:2586–2590.
90. Berlman, I. B., 1973, Empirical study of heavy-atom collisional quenching of the fluorescence state of aromatic compounds in solution, *J. Phys. Chem.* **77**:562–567.
91. James, D. R., and Ware, W. R., 1985, Multiexponential fluorescence decay of indole-3-alkanoic acids, *J. Phys. Chem.* **89**:5450–5458.
92. Illsley, N. P., and Verkman, A. S., 1987, Membrane chloride transport measured using a chloride-sensitive fluorescent probe, *Biochemistry* **26**:1215–1219.
93. Chao, A. C., Dix, J. A., Sellers, M. C., and Verkman, A. S., 1989, Fluorescence measurement of chloride transport in monolayer cultured cells, *Biophys. J.* **56**:1071–1081.
94. Verkman, A. S., 1990, Development and biological applications of chloride-sensitive fluorescent indicators, *Am. J. Phys.* **253**:C375–C388.
95. Martin, A., and Narayanaswamy, R., 1997, Studies on quenching of fluorescence of reagents in aqueous solution leading to an optical chloride-ion sensor, *Sensors Actuators B* **38–39**:330–333.
96. Daems, D., Boens, N., and Schryver, F. C., 1989, Fluorescence quenching with lindane in small unilamellar L-α-dimyristoylphosphatidylcholine vesicles, *Eur. Biophys. J.* **17**:25–36.
97. Namiki, A., Nakashima, N., and Yoshihara, K., 1979, Fluorescence quenching due to the electron transfer. Indole-chloromethanes in rigid ethanol glass, *J. Chem. Phys.* **71**:925–930.
98. Johnson, G. E., 1980, Fluorescence quenching of carbazoles, *J. Phys. Chem.* **84**:2940–2946.
99. Jones, G. T., and Lee, A. G., 1985, Interactions of hexachlorocyclohexanes with lipid bilayers, *Biochim. Biophys. Acta* **812**:731–739.
100. Hariharan, C., Vijayaree, V., and Mishra, A. K., 1997, Quenching of 2,5-diphenyloxazole (PPO) fluorescence by metal ions, *J. Lumin.* **75**:205–211.
101. Morris, S. J., Bradley, D., and Blumenthal, R., 1985, The use of cobalt ions as a collisional quencher to probe surface charge and stability of fluorescently labeled bilayer vesicles, *Biochim. Biophys. Acta* **818**:365–372.
102. Homan, R., and Eisenberg, M., 1985, A fluorescence quenching technique for the measurement of paramagnetic ion concentrations at the membrane/water interface. Intrinsic and X537A-mediated cobalt fluxes across lipid bilayer membranes, *Biochim. Biophys. Acta* **812**:485–492.
103. Salthammer, T., Dreeskamp, H., Birch, D. J. S., and Imhof, R. E., 1990, Fluorescence quenching of perylene by Co^{2+} ions via energy transfer in viscous and non-viscous media, *J. Photochem. Photobiol., A: Chem.* **55**:53–62.
104. Holmes, A. S., Birch, D. J. S., Suhling, K., Imhof, R. E., Salthammer, T., and Dreeskamp, H., 1991, Evidence for donor–donor energy transfer in lipid bilayers: Perylene fluorescence quenching by Co^{2+} ions, *Chem. Phys. Lett.* **186**:189–194.
105. Birch, D. J. S., Suhling, K., Holmes, A. S., Salthammer, T., and Imhof, R. E., 1992, Fluorescence energy transfer to metal ions in lipid bilayers, *Proc. SPIE* **1640**:707–718.
106. Perochon, E., and Tocanne, J.-F., 1991, Synthesis and phase properties of phosphatidylcholine labeled with 8-(2-anthroyl)octanoic acid, a solvatochromic fluorescent probe, *Chem. Phys. Lipids* **58**:7–17.
107. Pucaloro, A. F., Forster, L. S., and Campbell, M. K., 1984, Fluorescence quenching of indole by dimethylformamide, *Photochem. Photobiol.* **39**:503–506.
108. Swadesh, J. K., Mui, P. W., and Scheraga, H. A., 1987, Thermodynamics of the quenching of tyrosyl fluorescence by dithiothreitol, *Biochemistry* **26**:5761–5769.
109. Valentino, M. R., and Boyd, M. K., 1995, Ether quenching of singlet excited 9-arylxanthyl cations, *J. Photochem. Photobiol.* **89**:7–12.
110. Medinger, T., and Wilkinson, F., 1965, Mechanism of fluorescence quenching in solution I. Quenching of bromobenzene, *Trans. Faraday Soc.* **61**:620–630.
111. Ahmad, A., and Durocher, G., 1981, How hydrogen bonding of carbazole to ethanol affects its fluorescence quenching rate by electron acceptor quencher molecules, *Photochem. Photobiol.* **34**:573–578.
112. Bowen, E. J., and Metcalf, W. S., 1951, The quenching of anthracene fluorescence, *Proc. R. Soc. London* **206A**:437–447.
113. Schmidt, R., Janssen, W., and Brauer, H.-D., 1989, Pressure effect on quenching of perylene fluorescence by halonaphthalenes, *J. Phys. Chem.* **93**:466–468.
114. Encinas, M. V., Rubio, M. A., and Lissi, E., 1983, Quenching and photobleaching of excited polycyclic aromatic hydrocarbons by carbon tetrachloride and chloroform in micellar systems, *Photochem. Photobiol.* **37**:125–130.
115. Behera, P. K., Mukherjee, T., and Mishra, A. K., 1995, Quenching of substituted naphthalenes fluorescence by chloromethanes, *J. Lumin.* **65**:137–142.
116. Behera, P. K., and Mishra, A. K., 1993, Static and dynamic model for 1-naphthol fluorescence quenching by carbon tetrachloride in dioxane–acetonitrile mixtures, *J. Photochem. Photobiol., A: Chem.* **71**:115–118.
117. Behera, P. K., Mukherjee, T., and Mishra, A. K., 1995, Simultaneous presence of static and dynamic component in the fluorescence quenching for substituted naphthalene–CCl_4 systems, *J. Lumin.* **65**:131–136.
118. Zhang, J., Rork, D. P., Chateauneuf, J. E., and Brennecke, J. F., 1997, A steady-state and time-resolved fluorescence study of quenching reactions of anthracene and 1,2-benzanthracene by carbon tetrabromide and bromoethane in supercritical carbon dioxide, *J. Amer. Chem. Soc.* **119**:9980–9991.
119. Tucker, S. A., Cretella, L. E., Waris, R., Street, K. W., Acree, W. E., and Fetzer, J. C., 1990, Polycyclic aromatic hydrocarbon solute probes. Part VI: Effect of dissolved oxygen and halogenated sol-

vents on the emission spectra of select probe molecules, *Appl. Spectrosc.* 44:269–273.
120. Wiczk, W. M., and Latowski, T., 1992, The effect of temperature on the fluorescence quenching of perylene by tetrachloromethane in mixtures with cyclohexane and benzene, *Z. Naturforsch. A* 47:533–535.
121. Wiczk, W. M., and Latowski, T., 1986, Photophysical and photochemical studies of polycyclic aromatic hydrocarbons in solutions containing tetrachloromethane. I. Fluorescence quenching of anthracene by tetrachloromethane and its complexes with benzene, *p*-xylene and mesitylene, *Z. Naturforsch. A* 41:761–766.
122. Goswami, D., Sarpal, R. S., and Dogra, S. K., 1991, Fluorescence quenching of few aromatic amines by chlorinated methanes, *Bull. Chem. Soc. Jpn.* 64:3137–3141.
123. Takahashi, T., Kikuchi, K., and Kokubun, H., 1980, Quenching of excited 2,5-diphenyloxazole by CCl_4, *J. Photochem.* 14:67–76.
124. Alford, P. C., Cureton, C. G., Lampert, R. A., and Phillips, D., 1983, Fluorescence quenching of tertiary amines by halocarbons, *Chem. Phys.* 76:103–109.
125. Khwaja, H. A., Semeluk, G. P., and Unger, I., 1984, Quenching of the singlet and triplet state of benzene in condensed phase, *Can. J. Chem.* 62:1487–1491.
126. Washington, K., Sarasua, M. M., Koehler, L. S., Koehler, K. A., Schultz, J. A., Pedersen, L. G., and Hiskey, R. G., 1984, Utilization of heavy-atom effect quenching of pyrene fluorescence to determine the intramembrane distribution of halothane, *Photochem. Photobiol.* 40:693–701.
127. Lopez, M. M., and Kosk-Kosicka, D., 1998, Spectroscopic analysis of halothane binding to the plasma membrane Ca^{2+}-ATPase, *Biophys. J.* 74:974–980.
128. Cavatorta, P., Favilla, R., and Mazzini, A., 1979, Fluorescence quenching of tryptophan and related compounds by hydrogen peroxide, *Biochim. Biophys. Acta* 578:541–546.
129. Vos, R., and Engelborghs, Y., 1994, A fluorescence study of tryptophan–histidine interactions in the peptide alanin and in solution, *Photochem. Photobiol.* 60:24–32.
130. Mae, M., Wach, A., and Najbar, J., 1991, Solvent effects on the fluorescence quenching of anthracene by iodide ions, *Chem. Phys. Lett.* 176:167–172.
131. Blatt, E., Ghiggino, K. P., and Sawyer, W. H., 1982, Fluorescence depolarization studies of *n*-(9-anthroyloxy) fatty acids in cetyltrimethylammonium bromide micelles, *J. Phys. Chem.* 86:4461–4464.
132. Fraijl, L. K., Hayes, D. M., and Werner, T. C., 1992, Static and dynamic fluorescence quenching experiments for the physical chemistry laboratory, *J. Chem. Educ.* 69:424–428.
133. Zhu, C., Bright, F. V., and Hieftje, G. M., 1990, Simultaneous determination of Br^- and I^- with a multiple fiber-optic fluorescence sensor, *Appl. Spectrosc.* 44:59–64.
134. Lakowicz, J. R., and Anderson, C. J., 1980, Permeability of lipid bilayers to methylmercuric chloride: Quantification by fluorescence quenching of a carbazole-labeled phospholipid, *Chem.-Biol. Interact.* 30:309–323.
135. Boudou, A., Desmazes, J. P., and Georgescauld, D., 1982, Fluorescence quenching study of mercury compounds and liposome interactions: Effect of charged lipid and pH, *Ecotoxicol. Environ. Saf.* 6:379–387.
136. Holmes, A. S., Suhling, K., and Birch, D. J. S., 1993, Fluorescence quenching by metal ions in lipid bilayers, *Biophys. Chem.* 46:193–204.
137. Birch, D. J. S., Suhling, K., Holmes, A. S., Salthammer, T., and Imhof, R. E., 1993, Metal ion quenching of perylene fluorescence in lipid bilayers, *Pure Appl. Chem.* 65:1687–1692.
138. Sawicki, E., Stanley, T. W., and Elbert, W. C., 1964, Quenchofluorometric analysis for fluoranthenic hydrocarbons in the presence of other types of aromatic hydrocarbon, *Talanta* 11:1433–1441.
139. Dreeskamp, H., Koch, E., and Zander, M., 1975, On the fluorescence quenching of polycyclic aromatic hydrocarbons by nitromethane, *Z. Naturforsch. A* 30:1311–1314.
140. Pandey, S., Fletcher, K. A., Powell, J. R., McHale, M. E. R., Kaupplia, A-S. M., Acree, W. E., Fetzer, J. C., Dai, W., and Harvey, R. G., 1997, Spectrochemical investigations of fluorescence quenching agents. Part 5. Effect of surfactants on the ability of nitromethane to selectively quench fluorescence emission of alternant PAHs, *Spectrochim. Acta, Part A* 53:165–172.
141. Pandey, S., Acree, W. E., Cho, B. P., and Fetzer, J. C., 1997, Spectroscopic properties of polycyclic aromatic compounds. Part 6. The nitromethane selective quenching rule visited in aqueous micellar zwitterionic surfactant solvent media, *Talanta* 44:413–421.
142. Acree, W. E., Pandey, S., and Tucker, S. A., 1997, Solvent-modulated fluorescence behavior and photophysical properties of polycyclic aromatic hydrocarbons dissolved in fluid solution, *Curr. Top. Solution Chem.* 2:1–27.
143. Tucker, S. A., Acree, W. E., Tanga, M. J., Tokita, S., Hiruta, K., and Langhals, H., 1992, Spectroscopic properties of polycyclic aromatic compounds: Examination of nitromethane as a selective fluorescence quenching agent for alternant polycyclic aromatic nitrogen hetero-atom derivatives, *Appl. Spectrosc.* 46:229–235.
144. Tucker, S. A., Acree, W. E., and Upton, C., 1993, Polycyclic aromatic nitrogen heterocycles. Part V: Fluorescence emission behavior of select tetraaza- and diazaarenes in nonelectrolyte solvents, *Appl. Spectrosc.* 47:201–206.
145. Green, J. A., Singer, L. A., and Parks, J. H., 1973, Fluorescence quenching by the stable free radical di-*t*-butylnitroxide, *J. Chem. Phys.* 58:2690–2695.
146. Bieri, V. G., and Wallach, D. F. H., 1975, Fluorescence quenching in lecithin:cholesterol liposomes by paramagnetic lipid analogues: Introduction of new probe approach, *Biochim. Biophys. Acta* 389:413–427.
147. Encinas, M. V., Lissi, E. A., and Alvarez, J., 1994, Fluorescence quenching of pyrene derivatives by nitroxides microheterogeneous systems, *Photochem. Photobiol.* 59:30–34.
148. Matko, J., Ohki, K., and Edidin, M., 1992, Luminescence quenching by nitroxide spin labels in aqueous solution: Studies on the mechanism of quenching, *Biochemistry* 31:703–711.
149. Jones, P. F., and Siegel, S., 1971, Quenching of naphthalene luminescence by oxygen and nitric oxide, *J. Chem. Phys.* 54:3360–3366.
150. Harper, J., and Sailor, M. J., 1996, Detection of nitric oxide and nitrogen dioxide with photoluminescent porous silicon, *Anal. Chem.* 68:3713–3717.
151. Denicola, A., Souza, J. M., Radi, R., and Lissi, E., 1996, Nitric oxide diffusion in membranes determined by fluorescence quenching, *Arch. Biochem. Biophys.* 328:208–212.
152. Ware, W. R., Holmes, J. D., and Arnold, D. R., 1974, Exciplex photophysics. II. Fluorescence quenching of substituted anthracenes by substituted 1,1-diphenylethylenes, *J. Am. Chem. Soc.* 96:7861–7864.
153. Labianca, D. A., Taylor, G. N., and Hammond, G. S., 1972, Structure–reactivity factors in the quenching of fluorescence from naphthalenes by conjugated dienes, *J. Am. Chem. Soc.* 94:3679–3683.
154. Encinas, M. V., Guzman, E., and Lissi, E. A., 1983, Intramolecular aromatic hydrocarbon fluorescence quenching by olefins, *J. Phys. Chem.* 87:4770–4772.

155. Abuin, E. B., and Lissi, E. A., 1993, Quenching rate constants in aqueous solution: Influence of the hydrophobic effect, *J. Photochem. Photobiol.* 71:263–267.
156. Chang, S. L. P., and Schuster, D. I., 1987, Fluorescence quenching of 9,10-dicyanoanthracene by dienes and alkenes, *J. Phys. Chem.* 91:3644–3649.
157. Eriksen, J., and Foote, C. S., 1978, Electron-transfer fluorescence quenching and exciplexes of cyano-substituted anthracenes, *J. Phys. Chem.* 82:2659–2662.
158. Fischkoff, S., and Vanderkooi, J. M., 1975, Oxygen diffusion in biological and artificial membranes determined by the fluorochrome pyrene, *J. Gen. Phys.* 65:663–676.
159. Jameson, D. M., Gratton, E., Weber, G., and Alpert, B., 1984, Oxygen distribution and migration within $MB^{DES\ PE}$ and $HB^{DES\ PE}$, *Biophys. J.* 45:795–803.
160. Subczynski, W. K., Hyde, J. S., and Kusumi, A., 1989, Oxygen permeability of phosphatidylcholine-cholesterol membranes, *Proc. Natl. Acad. Sci. U.S.A.* 86:4474–4478.
161. Damas, D., Muller, S., Gonis, F., Baros, F., Viriot, M.-L., and Stoltz, J.-F., 1997, Membrane fluidity and oxygen diffusion in cholesterol-enriched erythrocyte membrane, *Arch. Biochem. Biophys.* 341:34–39.
162. Czarnyshan, S. V., Gritsan, N. P., Korolev, V. V., and Bazhin, N. M., 1990, Quenching of the luminescence of organic compounds by oxygen in glassy matrices, *Chem. Phys.* 142:59–68.
163. Kikuchi, K., Sato, C., Watabe, M., Ikeda, H., Takahashi, Y., and Miyashi, T., 1993, New aspects on fluorescence quenching by molecular oxygen, *J. Am. Chem. Soc.* 115:5180–5184.
164. Vaughan, W. M., and Weber, G., 1970, Oxygen quenching of pyrenebutyric acid fluorescence in water. A dynamic probe of the microenvironment, *Biochemistry* 9:464–473.
165. Abuin, E. B., and Lissi, E. A., 1991, Diffusion and concentration of oxygen in microheterogeneous systems. Evaluation from luminescence quenching data, *Prog. React. Kinet.* 16:1–33.
166. Parasassi, T., and Gratton, E., 1992, Packing of phospholipid vesicles studied by oxygen quenching of laurdan fluorescence, *J. Fluoresc.* 2:167–174.
167. Encinas, M. V., and Lissi, E. A., 1983, Intramicellar quenching of 2,3-dimethylnaphthalene fluorescence by peroxides and hydroperoxides, *Photochem. Photobiol.* 37:251–255.
168. Holmes, L. G., and Robbins, F. M., 1974, Quenching of tryptophyl fluorescence in proteins by *N*'-methylnicotinamide chloride, *Photochem. Photobiol.* 19:361–366.
169. Martin, M. M., and Wine, W. R., 1978, Fluorescence quenching of carbazole by pyridine and substituted pyridines. Radiationless processes in the carbazole–amine hydrogen bonded complex, *J. Phys. Chem.* 82:2770–2776.
170. Seely, G. R., 1978, The energetics of electron-transfer reactions of chlorophyll and other compounds, *Photochem. Photobiol.* 27:639–654.
171. Schroeder, J., and Wilkinson, F., 1979, Quenching of triplet states of aromatic hydrocarbons by quinones due to favourable charge-transfer interactions, *J. Chem. Soc., Faraday Trans. 2* 75:896–904.
172. Dreeskamp, H., Lauffer, A., and Zander, M., 1983, Löschung der perylen-fluoreszenz durch Ag^+-ionen, *Z. Naturforsch. A* 38:698–700.
173. Badley, R. A., 1975, The location of protein in serum lipoproteins: A fluorescence quenching study, *Biochim. Biophys. Acta* 379:517–528.
174. Eftink, M. R., and Ghiron, C. A., 1984, Indole fluorescence quenching studies on proteins and model systems: Use of the inefficient quencher succinimide, *Biochemistry* 23:3891–3899.
175. Moore, H.-P. H., and Raftery, M. A., 1980, Direct spectroscopic studies of cation translocation by *Torpedo* acetylcholine receptor on a time scale of physiological relevance, *Proc. Natl. Acad. Sci. U.S.A.* 77:4509–4513.
176. Mac, M., Najbar, J., Phillips, D., and Smith, T. A., 1992, Solvent dielectric relaxation properties and the external heavy atom effect in the time-resolved fluorescence quenching of anthracene by potassium iodide and potassium thiocyanate in methanol and ethanol, *J. Chem. Soc., Faraday Trans.* 88:3001–3005.
177. Carrigan, S., Doucette, S., Jones, C., Marzzacco, C. J., and Halpern, A. M., 1996, The fluorescence quenching of 5,6-benzoquinoline and its conjugate acid by Cl^-, Br^-, SCN^- and I^- ions, *J. Photochem. Photobiol., A: Chem.* 99:29–35.
178. Horrocks, A. R., Kearvell, A., Tickle, K., and Wilkinson, F., 1966, Mechanism of fluorescence quenching in solution II. Quenching by xenon and intersystem crossing efficiencies, *Trans. Faraday Soc.* 62:3393–3399.

PROBLEMS

8.1. *Separation of Static and Dynamic Quenching of Acridone by Iodide*: The following data were obtained for quenching of acridone in water at 26 °C.[78] KNO_3 is used to maintain a constant ionic strength and does not quench the fluorescence of acridone.

[KI] (*M*)	$[KNO_3]$ (*M*)	F_0/F
0.0	1.10	[1.0]
0.04	1.06	4.64
0.10	1.00	10.59
0.20	0.90	23.0
0.30	0.80	37.2
0.50	0.60	68.6
0.80	0.30	137

A. Construct a Stern–Volmer plot.
B. Determine the dynamic (K_D) and static (K_S) quenching constants. Use the quadratic equation to obtain K_D and K_S from the slope and intercept of a plot of K_{app} versus [Q].
C. Calculate the observed bimolecular quenching constant. The unquenched lifetime $\tau_0 = 17.6$ ns.
D. Calculate the diffusion-limited bimolecular quenching constant and the quenching efficiency. The diffusion constant of KI in water is 2.065×10^{-5} cm^2/s for 1*M* KI (*Handbook of Chemistry and Physics*, 55th ed.).
E. Comment on the magnitude of the sphere of action and the static quenching constant, with regard to the nature of the complex.

8.2. *Separation of Static and Dynamic Quenching*: The following table lists the fluorescence lifetimes and relative quantum yields of 10-methylacridinium chloride (MAC) in the presence of adenosine monophosphate (AMP).[18]

[AMP] (m*M*)	τ (ns)	Intensity
0	32.9	1.0
1.75	26.0	0.714
3.50	21.9	0.556
5.25	18.9	0.426
7.00	17.0	0.333

A. Is the quenching dynamic, static, or both?
B. What is (are) the quenching constant(s)?
C. What is the association constant for the MAC–AMP complex?
D. Comment on the magnitude of the static quenching constant.
E. Assume that the AMP–MAC complex is completely nonfluorescent and that complex formation shifts the absorption spectrum of MAC. Will the corrected excitation spectrum of MAC, in the presence of nonsaturating amounts of AMP, be comparable to the absorption spectrum of MAC or that of the MAC–AMP complex?

8.3. *Effects of Dissolved Oxygen on Fluorescence Intensities and Lifetimes*: Oxygen is known to dissolve in aqueous and organic solutions and is a collisional quencher of fluorescence. Assume that your measurements are accurate to 3%. What are the lifetimes above which dissolved oxygen from the atmosphere will result in changes in the fluorescence intensities or lifetimes that are outside your accuracy limits? Indicate these lifetimes for both aqueous and ethanolic solutions. The oxygen solubility in water is 0.001275*M* for a partial pressure of 1 atm. Oxygen is fivefold more soluble in ethanol than in water. The following information is needed to answer this question: k_q (in water) = $1 \times 10^{10}\ M^{-1}\ s^{-1}$; k_q (in ethanol) = $2 \times 10^{10}\ M^{-1}\ s^{-1}$.

8.4. *Intramolecular Complex Formation by Flavin Adenine Dinucleotide (FAD)*: FAD fluorescence is quenched both by static complex formation between the flavin and adenine rings and by collisions between these two moieties. Flavin mononucleotide (FMN) is similar to FAD except that it lacks the adenine ring. Use the following data for FAD and FMN to calculate the fraction complexed (f) and the collisional deactivation rate (k) of the flavin by the adenine ring. Q is the relative quantum yield. Note that the deactivation rate is in units of s^{-1}.
τ (FMN) = 4.6 ns
τ (FAD) = 2.4 ns
Q(FMN) = 1.0 (assumed unity)
Q(FAD) = 0.09

8.5. *Quenching of Protein Fluorescence; Determination of the Fraction of the Total Fluorescence Accessible to Iodide:* Assume that a protein contains four identical subunits, each containing two tryptophan residues. The following data are obtained in the presence of iodide.

$[I^-]$ (*M*)	Fluorescence intensity
0.00	1.0
0.01	0.926
0.03	0.828
0.05	0.767
0.10	0.682
0.20	0.611
0.40	0.563

A. What fraction of the total tryptophan fluorescence is accessible to quenching?
What property of the Stern–Volmer plots indicates an inaccessible fraction?
B. Assume that all the tryptophans have equal quantum yields and lifetimes (5 ns). How many tryptophan residues are accessible to quenching?
C. What are the bimolecular quenching constants for the accessible and inaccessible residues?
D. Assume that you could selectively excite the accessible tryptophans by excitation at 300 nm. Draw the predicted Stern–Volmer and modified Stern–Volmer plots for the accessible and the inaccessible residues.

8.6. *Quenching of Endonuclease III:* Figure 8.39 shows the effect of a 19-mer of poly(dA-dT) on the intrinsic tryptophan emission of endo nuclease III (Endo III). Explain the data in terms of the structure of endo III (Figure 8.15). Is the quenching collisional or static? Assume that the unquenched decay time is 5 ns. The concentration of endo III is 0.8μ*M*.

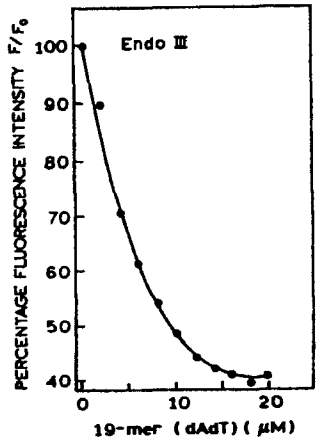

Figure 8.39. Fluorescence intensity of endo III with increasing concentrations of a 19-mer of poly(dA-dT). Revised from Ref. 40.